Singularity avoidance for collapsing quantum dust in the Lemaître-Tolman-Bondi model

Claus Kiefer* and Tim Schmitz†

Institut für Theoretische Physik, Universität zu Köln, Zülpicher Straße 77, 50937 Köln, Germany

(Received 6 May 2019; published 14 June 2019)

We investigate the fate of the classical singularity in a collapsing dust cloud. For this purpose, we quantize the marginally bound Lemaître-Tolman-Bondi model for spherically symmetric dust collapse by considering each dust shell in the cloud individually, taking the outermost shell as a representative. Because the dust naturally provides a preferred notion of time, we can construct a quantum mechanical model for this shell and demand unitary evolution for wave packets. It turns out that the classical singularity can generically be avoided provided the quantization ambiguities fulfill some weak conditions. We demonstrate that the collapse to a singularity is replaced by a bounce followed by an expansion. We finally construct a quantum corrected spacetime describing bouncing dust collapse and calculate the time from collapse to expansion.

DOI: 10.1103/PhysRevD.99.126010

I. INTRODUCTION

It is an open problem whether the ubiquitous singularities of general relativity will disappear after quantization. Since there is no consensus so far on the appropriate quantum theory of gravity, this question can be decided only within a given approach and for certain classes of models.

In this paper, we shall address the fate of the classical singularity for a collapsing dust cloud. The framework will be quantum geometrodynamics, which is the canonical formulation based on metric variables. Although this approach may not be the most fundamental one, it is a conservative approach: one can arrive at the quantum constraint equations by devising wave equations from which the classical Einstein equations follow in the semiclassical (WKB) limit [1].

There already exist various results on the fate of singularities for collapsing spherically symmetric dust *shells*. Using an effective one-loop action with an Einstein-Hilbert term plus a Weyl tensor-squared term, it was found that a thin null dust shell collapses and reexpands instead of ending in a black hole (BH) singularity [2]. In quantum geometrodynamics, the quantization of a collapsing dust shell was discussed in a mathematically rigorous way in [3–5], see also [6] for a review. The demand for a unitary evolution leads to a wave *vanishing* at the origin, that is, at the place (more precisely, the time) where classically the singularity sits. The shell, if represented by a wave packet, collapses to a minimal radius inside its horizon and then reexpands. In the classical theory, this reexpanding wave packet corresponds to a white hole. That the singularity is avoided in this way is not surprising. In a unitary time evolution it is not possible that the wave packet *disappears* in a singularity—it must reexpand.

A different but related situation arises for quantum cosmological models. There, unitarity does not hold for the standard Wheeler-DeWitt equation [1]. It is, however, possible to impose the "DeWitt criterion" of vanishing wave function in the limit of approaching the classical cosmological singularity. This was investigated for several models; see, for example, [7] and the references therein. Recently, the DeWitt criterion was generalized in order to accommodate the conformal nature of the configuration space [8].

Concerning the fate of collapsing dust shells, there are also investigations in other approaches, notably from loop quantum gravity [9–12]. Again, collapsing quantum shells turn into expanding ones. A major issue there is the question of the lifetime of the BH-like temporary object and the behavior of the horizon. This is of great importance for relating theses scenarios to potential observations. They provide realistic models only if the lifetime is bigger than the current age of our Universe. Otherwise, they cannot be applied to describing the quantum collapse of astrophysical objects such as supernovae.

Concerning the details of the scenario, there are a variety of ideas available: the horizon could, for example, disappear during the bounce [12–15] or could be in a superposition of BH and white hole (WH) horizons, with a smooth transition between the two in the form of a "grey horizon" [3]. There have also been different pictures about the detailed mechanism that leads to the quantum effects at the horizon, a spacetime region in which the curvature is

*kiefer@thp.uni-koeln.de
†tschmitz@thp.uni-koeln.de

usually low. Haggard and Rovelli, for example, envision an accumulation of quantum effects over time [16], while Barceló *et al.* propose a shockwave propagating outward from the would-be singularity [14,15]. There is also little consensus about the lifetime, different approaches to the problem giving different results [5,17–19]. A recent review is given in [20].

In this paper, we shall discuss these problems for the inhomogeneous spherically symmetric dust collapse described by the Lemaître-Tolman-Bondi (LTB) model; see, for example, [21] for a presentation of the classical LTB model. Its quantization in the geometrodynamical context was presented in [22,23]. While it was possible in this model to recover Hawking radiation [24], to compute nonthermal corrections to it [25,26], and to investigate BH entropy and the BH mass spectrum [27], the question of singularity avoidance could not be settled. The main reason for this failure is the inhomogeneous nature of a dust cloud and the ensuing functional form of the quantum constraints. Similarly, while it was claimed that in spherically symmetric loop quantum gravity the singularity is avoided due to the fundamentally quantized nature of space [28,29], investigating different loop quantum gravity inspired corrections to the LTB model has not suggested any particular mechanism for this avoidance; a singularity seems to form just as it does classically [30,31].

Here, we shall develop a different approach to quantizing the LTB model. The idea is to consider each shell individually, sidestepping some technical and conceptual difficulties, and try to infer the behavior of the full dust cloud from our results. This will enable us to tackle the question of singularity avoidance and to suggest a scenario with a bounce as the typical behavior of the quantized dust cloud. Singularities can thus be avoided. This bounce is a direct consequence of the unitary evolution with respect to dust proper time.

Our paper is organized as follows. In Sec. II we introduce the reader to the LTB model and lay the classical foundations for our approach. We then develop and investigate the corresponding quantum theory in Sec. III, first making general statements about its states, and then examining a specific one in the form of a wave packet. Based on the dynamics of this wave packet, we construct a quantum corrected space time for dust collapse and discuss some of its properties in Sec. IV. We discuss, in particular, the lifetime for the wave packet to collapse and reexpand. Section V contains our conclusions.

II. THE CLASSICAL LTB MODEL AND ITS ON-SHELL ACTION

We give here a brief introduction to the LTB model. It is a spherically symmetric solution of the Einstein equations with nonrotating dust of mass density ϵ as its source. Its line element reads

$$ds^2 = -c^2 d\tau^2 + \frac{R'^2}{1+2f} d\rho^2 + R^2 d\Omega^2, \tag{1}$$

$$\text{with} \quad \frac{8\pi G}{c^2}\epsilon = \frac{F'}{R^2 R'} \quad \text{and} \quad \frac{\dot{R}^2}{c^2} = \frac{F}{R} + 2f. \tag{2}$$

A prime (dot) denotes a derivative with respect to ρ (τ). The cosmological constant is set to zero. For the time coordinate one chooses the dust proper time τ and for the radial coordinate the variable ρ, which continuously labels the spherically symmetric dust shells at fixed τ. In the following, we shall set $G = 1 = c$.

In these units, $F(\rho)$ is twice the Misner-Sharp mass (see e.g., [32], page 40) for the LTB spacetime, which gives the active gravitating mass that is contained in the shell with label ρ. From the condition $R(\tau,\rho) = F(\rho)$ one can also infer whether a shell coincides with an apparent horizon; the horizon can be future or past depending on the sign of $\dot{R}$. The energy function $f(\rho)$ plays a role for the general LTB model, but for simplicity we will in the following restrict ourselves to the marginally bound LTB model for which $f = 0$.

An important quantity is $R(\tau,\rho)$, which is the curvature radius of the shell labeled by ρ at time τ; it describes how the dust shells collapse or expand. A central or shell focusing singularity forms in the LTB model when shells collapse to the point $R = 0$.

In addition to the central singularity also shell crossing singularities can appear. They occur when two dust shells occupy the same radius, that is, when $R' = 0$. They are generally assumed to be an artifact of using a simplistic matter model and hence are considered unphysical. We will not address these singularities here, because one can choose initial conditions such that they do not occur. Moreover, it is possible to extend the spacetime beyond them; see [33,34] and the references therein.

We emphasize that the equation of motion relevant for R, the second equation in (2), only depends on R and F (and also on f for the nonmarginally bound case), but not on their spatial derivatives. When a mass function is given, different dust shells are decoupled, as they do not dynamically influence each other.

Based on this decoupling, we can consider the different shells in the LTB model independently. Consequently, we will quantize a single shell in the marginally bound LTB model and then try to deduce the dynamics of the full dust cloud. In the following, we will derive a Hamiltonian for the outermost dust shell.

We start from the Einstein-Hilbert action

$$S = \frac{1}{16\pi}\int_{\mathcal{M}} d^4x\sqrt{-g}\mathcal{R}[g] + \frac{1}{8\pi}\int_{\partial\mathcal{M}} d^3x\eta\sqrt{|h|}(k-k^0), \tag{3}$$

and insert a marginally bound LTB solution in the coordinates (τ,ρ,θ,ϕ), where the angular coordinates can be

integrated out immediately. In (3), k is the trace of the extrinsic curvature of $\partial\mathcal{M}$, and k^0 is the same quantity for the case that this hypersurface is embedded into flat space. The factor η is equal to 1 when $\partial\mathcal{M}$ is timelike and -1 when it is spacelike [35].

For the boundary $\partial\mathcal{M}$ of the spacetime $\mathcal{M}$ we take $\partial\mathcal{M} = \mathcal{B}_o \cup \mathcal{B}_{\tau_1} \cup \mathcal{B}_{\tau_2}$, where $\mathcal{B}_{\tau_{1/2}}$ are spacelike hypersurfaces of fixed constant dust proper time with $\tau_1 < \tau_2$, and $\mathcal{B}_o$ is the timelike boundary coinciding with the worldtube of the outermost dust shell $\rho = \rho_o$. We will mostly not concern ourselves with the geometry outside the cloud, although one can always attach a Schwarzschild exterior with mass $M = \frac{1}{2}F(\rho_o) =: \frac{1}{2}F_o$. Below we will refer to F_o (twice the mass contained in the outermost shell) as twice the Arnowitt-Deser-Misner (ADM) energy of the dust cloud, $2E_{\mathrm{ADM}}$, always with this exterior geometry in mind.

Taking the trace of the Einstein equations for LTB gives

$$\sqrt{-g}\mathcal{R}[g] = 8\pi\epsilon R^2 R' \sin\theta = F' \sin\theta,$$

where we have used the equations of motion (2). This gives for the bulk part of the action (3), $S_{\mathcal{M}}$, the expression

$$S_{\mathcal{M}} = \frac{1}{4}\int d\tau \int_0^{\rho_o} d\rho F' = \frac{1}{4}\int d\tau F_o = \frac{1}{4}\int d\tau R_o \dot{R}_o^2,$$

where R_o denotes the radius of the outermost shell. We have made here the assumption that the innermost shell contains no mass, $F(0) = 0$, and have used the remaining part of (2).

Now we turn to the boundary terms. Calculating the trace of the extrinsic curvature of the timelike boundary $\mathcal{B}_o$ gives

$$k_o = \frac{2}{R}.$$

Since this matches the trace of the extrinsic curvature for the same hypersurface embedded into flat space, k_o^0, the corresponding boundary term in (3) vanishes. Note that the same would hold for a boundary term at the innermost shell $\rho = 0$.

Let us now calculate the contributions from the temporal boundaries. The trace of the extrinsic curvature of the $\tau = \text{const.}$ hypersurfaces is given by

$$k_\tau = \frac{\dot{R}'}{R'} + 2\frac{\dot{R}}{R},$$

while k_τ^0 simply vanishes. This gives

$$S_{\mathcal{B}_\tau} = -\frac{1}{2}\int_0^{\rho_o} d\rho (R^2\dot{R}' + 2RR'\dot{R}) = -\frac{1}{2}[R^2\dot{R}]_0^{\rho_o}.$$

Combining the two terms for τ_1 and τ_2 gives a more convenient form for these boundary contributions. One has to keep in mind that the normal to $\mathcal{B}_{\tau_1}$ is future directed, while the normal to $\partial\mathcal{M}$ is past directed in the region $\mathcal{B}_{\tau_1}$. The past-directed boundary term hence carries an additional sign -1 [35], giving

$$\begin{aligned} S_{\mathcal{B}_\tau}|_{\tau_1}^{\tau_2} &= -\frac{1}{2}[R^2\dot{R}|_{\tau_2} - R^2\dot{R}|_{\tau_1}]_0^{\rho_o} \\ &= -\frac{1}{2}\int d\tau \frac{\partial}{\partial\tau}[R^2\dot{R}]_0^{\rho_o} \\ &= -\frac{3}{4}\int d\tau [R\dot{R}^2]_0^{\rho_o} = -\frac{3}{4}\int d\tau R_o \dot{R}_o^2. \end{aligned}$$

Here we have used $R^2\ddot{R} = -\frac{1}{2}R\dot{R}^2$, which follows from the time independence of $F = R\dot{R}^2$.

The full action for an LTB solution of the outermost shell then reads

$$S = -\frac{1}{2}\int d\tau R_o \dot{R}_o^2. \tag{4}$$

We note that choosing Brown-Kuchař dust as the matter component, the dust action trivially vanishes on shell [36].

We have now arrived at an action that describes the dynamics of the outermost shell. This is not surprising, since we have already inserted the proper dynamics for the dynamical field $R(\rho)$ and are now left with a prescription for how the boundary conditions given at the initial time τ_1 are to be evolved into the future. In this sense, the above action (4) is an action for the outermost shell on the background of all other shells.

We note that including the boundary terms has only contributed to the prefactor of the action. If we neglected them, we would only find a different prefactor that would leave the classical dynamics unchanged and would only introduce minor changes to the quantum model below.

The momentum conjugate to R_o and the Hamiltonian corresponding to (4) then read, respectively,

$$P_o = -R_o\dot{R}_o, \tag{5}$$

$$H = -\frac{P_o^2}{2R_o}. \tag{6}$$

This Hamiltonian is the negative of the ADM energy,

$$H = -\frac{1}{2}R_o\dot{R}_o^2 = -\frac{1}{2}F_o = -E_{\mathrm{ADM}},$$

implying its conservation. It is then obvious that H gives the expected dynamics. Adjusting the constant of motion F_o, this Hamiltonian describes the dynamics of any single shell in the LTB model, not just the outermost one. It is also consistent with the on-shell Hamiltonian constraint for a marginally bound LTB model, see [30].

The fact that the Hamiltonian (6) is negative, although surprising at first glance, reflects the fact that the gravitational kinetic term in the Hamiltonian constraint is not positive definite (a feature that can be related to the attractivity of gravity [37]). As we have seen above, it is possible here to recover a positive notion of energy from it. A similar observation was made in [38], where phantom dust had to be used to recover a positive Hamiltonian for the LTB model.

We note that it is not possible to arrive at an action for nonmarginally bound LTB models in a similar way, but an effective Hamiltonian is easily constructed by simply adding a potential term fR, where f is constant for a given shell.

The Hamiltonian (6) also matches the gravitational Hamiltonian (with its negative kinetic term) for a flat Friedmann model with vanishing cosmological constant when identifying the scale factor as $ar_o = R_o$, where r_o is the parametric radius of the dust cloud [1]. When using Brown-Kuchař dust as matter and dust proper time as the time coordinate, the full Hamiltonian constraint for this Friedmann model reads $H + P_\tau = 0$, where P_τ is the momentum conjugate to τ [39]. Quantizing this constraint gives exactly the same Schrödinger equation as discussed below.

It follows that all results obtained in the following also apply to flat Friedmann models with vanishing cosmological constant. The same holds for models of (marginally bound) Oppenheimer-Snyder collapse, which shares its dynamics with these cosmological models.

III. QUANTUM DYNAMICS OF THE OUTERMOST SHELL

We will now apply the usual canonical quantization procedure in the Schrödinger representation to the Hamiltonian (6) by making the substitution

$$P_o \to \hat{P}_o = -i\hbar \frac{d}{dR_o}.$$

The operator $\hat{R}_o$ acts by multiplication. In the following we will suppress the subscript o.

The Hamiltonian then reads

$$\hat{H} = \frac{\hbar^2}{2} R^{-1+a+b} \frac{d}{dR} R^{-a} \frac{d}{dR} R^{-b}. \tag{7}$$

The parameters a and b describe our freedom of choosing a factor ordering. Two possible choices are distinguished. First, $a = b = 0$ corresponds to the naive factor ordering in which all derivatives are on the right. Second, $b = 0$ and $a = 1/2$ describes the Laplace-Beltrami ordering, which follows from the demand for covariance in configuration space. In the following we set $\hbar = 1$.

As a first step towards solving the τ-dependent Schrödinger equation

$$i\frac{\partial \Psi(R,\tau)}{\partial \tau} = \hat{H}\Psi(R,\tau)$$

with the Hamiltonian (7), we derive the stationary modes $\phi_E(R)$ satisfying $\hat{H}\phi_E = -E\phi_E$,

$$-E\phi_E = \frac{1}{2}\left(R^{-1+a+b}\frac{d}{dR}R^{-a}\frac{d}{dR}R^{-b}\right)\phi_E, \tag{8}$$

where E can be interpreted as E_{ADM}.

For $E > 0$, solutions of (8) are given by

$$\phi^1_E(R) = R^{\frac{1}{2}(1+a+2b)} J_{\frac{1}{3}|1+a|}\left(\frac{2}{3}\sqrt{2E}R^{\frac{3}{2}}\right), \tag{9}$$

$$\phi^2_E(R) = R^{\frac{1}{2}(1+a+2b)} Y_{\frac{1}{3}|1+a|}\left(\frac{2}{3}\sqrt{2E}R^{\frac{3}{2}}\right), \tag{10}$$

where $J_n(z)$ and $Y_n(z)$ are Bessel functions of the first and second kind, respectively.

The zero energy stationary modes are simpler,

$$\phi^1_0(R) = R^b, \qquad \phi^2_0(R) = \begin{cases} R^{1+a+b}, & a \neq -1 \\ R^b \ln R, & a = -1. \end{cases} \tag{11}$$

Although classically $E_{\mathrm{ADM}} \geq 0$, (8) also possesses solutions for negative energy. They can be interpreted as genuine quantum solutions without a classical counterpart. For this case, solutions are given by modified Bessel functions $I_n(z)$ and $K_n(z)$,

$$\phi^1_{-E}(R) = R^{\frac{1}{2}(1+a+2b)} I_{\frac{1}{3}|1+a|}\left(\frac{2}{3}\sqrt{2E}R^{\frac{3}{2}}\right), \tag{12}$$

$$\phi^2_{-E}(R) = R^{\frac{1}{2}(1+a+2b)} K_{\frac{1}{3}|1+a|}\left(\frac{2}{3}\sqrt{2E}R^{\frac{3}{2}}\right). \tag{13}$$

Note that in the following E will always be positive, and negative energy stationary states correspond to $-E$. We note that for the Laplace-Beltrami factor ordering, $a = 1/2$, the Bessel functions can be written as elementary functions.

We will construct the full quantum theory for our collapsing dust shell in analogy to ordinary quantum mechanics. We impose square integrability on wave functions and let them evolve unitarily according to a self-adjoint Hamiltonian. This corresponds to enforcing probability conservation in dust proper time. The treatment is similar in spirit to the treatment of the collapsing null dust shells in [4].

We start by choosing as the Hilbert space $L^2(\mathbb{R}^+, R^{1-a-2b}dR)$ the space of square integrable functions on the positive half line with respect to the scalar product:

$$\langle \phi, \psi \rangle = \int_0^\infty dR\, R^{1-a-2b} \phi^*(R)\psi(R).$$

The weight R^{1-a-2b} is fixed by the requirement that $\hat{H}$ be symmetric.[1] For Laplace-Beltrami ordering, the weight is just $\sqrt{R}$.

We note that we limit our discussion to stationary solutions of the Schrödinger equation and linear superpositions over different energies constructed from them, with wave packets in mind. This may exclude some wave functions if the stationary modes do not form a (generalized) basis of the functions we are interested in. Whether or not this is the case is hard to prove rigorously and will not be done here. We expect that the wave functions excluded by this restriction, should there be any, are not physically relevant.

A. Square integrability

We will now check which of the stationary modes (9)–(13) are square integrable with respect to our inner product. Obviously, the zero energy modes (11) are either not square integrable at $R = 0$ or at $R \to \infty$. The positive energy modes (9) and (10) are also not square integrable. This can be seen from the expansion of the Bessel functions for large arguments [40],

$$J_\nu(z) \sim \sqrt{\frac{2}{\pi z}} \cos\left(z - \frac{1}{2}\nu\pi - \frac{1}{4}\pi\right), \quad |\arg z| < \pi,$$
$$Y_\nu(z) \sim \sqrt{\frac{2}{\pi z}} \sin\left(z - \frac{1}{2}\nu\pi - \frac{1}{4}\pi\right), \quad |\arg z| < \pi.$$

It follows that the modes ϕ^1_E and ϕ^2_E approach infinity as

$$R^{\frac{1}{2}(1-a-2b)}\phi^1_E \sim \frac{R^{\frac{1}{4}}}{\sqrt{\frac{\pi}{3}}(2E)^{\frac{1}{4}}} \cos\left(\frac{2}{3}\sqrt{2E}R^{\frac{3}{2}} - \theta_a\right), \tag{14}$$

$$R^{\frac{1}{2}(1-a-2b)}\phi^2_E \sim \frac{R^{\frac{1}{4}}}{\sqrt{\frac{\pi}{3}}(2E)^{\frac{1}{4}}} \sin\left(\frac{2}{3}\sqrt{2E}R^{\frac{3}{2}} - \theta_a\right), \tag{15}$$

where $\theta_a = \frac{\pi}{6}|1+a| + \frac{\pi}{4}$. We note that in case of the Laplace-Beltrami factor ordering, this asymptotic behavior is exact for all R. That positive energy modes are not square integrable is not surprising. This is well known from, for example, the case of a free particle. The solutions are oscillatory and allow an interpretation in terms of Gel'fand triples (the factor $R^{\frac{1}{4}}$ does not prevent this). As in quantum mechanics, square integrability can be achieved by constructing wave packets.

We are now left with the negative energy modes (12) and (13). The expansion of the modified Bessel functions for large arguments reads [40]

$$I_\nu(z) \sim \frac{e^z}{\sqrt{2\pi z}}, \quad |\arg z| < \frac{\pi}{2}, \tag{16}$$

$$K_\nu(z) \sim \sqrt{\frac{\pi}{2z}} e^{-z}, \quad |\arg z| < \frac{3\pi}{2}. \tag{17}$$

We see that the mode ϕ^1_{-E} must be discarded because it diverges exponentially at infinity. As for ϕ^2_{-E}, it decreases exponentially at infinity, but we still have to check its behavior for $R \to 0$. For $z \to 0$ we have for the Bessel function,

$$K_\nu(z) \sim \begin{cases} \frac{\Gamma(\nu)}{2}\left(\frac{z}{2}\right)^{-\nu}, & \Re(\nu) > 0 \\ -\ln(z), & \nu = 0, \end{cases}$$

hence ϕ^2_{-E} approaches the singularity as

$$R^{\frac{1}{2}(1-a-2b)}\phi^2_{-E} \sim \begin{cases} \frac{\Gamma(\frac{1}{3}|1+a|)}{2(\frac{1}{3}\sqrt{2E})^{\frac{1}{3}|1+a|}} R^{1-\frac{1}{2}|1+a|}, & a \neq -1 \\ -R\ln\left(\frac{2}{3}\sqrt{2E}R^{\frac{3}{2}}\right), & a = -1. \end{cases} \tag{18}$$

It is thus square integrable also for $R \to 0$ if $|1+a| < 3$. Since it also decays exponentially at infinity, ϕ^2_{-E} is square integrable for these factor orderings.

B. Self-adjoint extensions of the Hamiltonian

We now want to find a domain for the Hamiltonian such that it is self-adjoint. Here, we will only state the results and refer to Appendix A for details.

For $|1+a| \geq 3$, the Hamiltonian is essentially self-adjoint and its unique domain is equal to what is called its natural domain, consisting of all square integrable functions ψ such that $\hat{H}\psi$ is square integrable as well (in addition to some continuity conditions).

Additional conditions emerge for $|1+a| < 3$. There we have a $U(1)$ family of self-adjoint extensions given by (A10),

$$-(1+e^{i\theta})R^{1-|1+a|}\frac{d}{dR}R^{-\frac{1}{2}(1+a-|1+a|+2b)}\psi\Big|_{R\to 0} = i(1-e^{i\theta})R^{1+|1+a|}\frac{d}{dR}R^{-\frac{1}{2}(1+a+|1+a|+2b)}\psi\Big|_{R\to 0} \tag{19}$$

for $a \neq -1$, and by

[1] One can also consider other weights of the form R^c with real parameters c. Instead of choosing a factor ordering that renders the Hamiltonian symmetric, equivalently to the above, one can construct a symmetrized Hamiltonian of the form $\frac{1}{2}(\hat{H} + \hat{H}^\dagger)$ (ignoring boundary terms). This leads to quantum theories equivalent to the one discussed here, but only if $\min\{1, -a\} \leq b + \frac{c}{2} \leq \max\{1, -a\}$. If this condition is not fulfilled, additional damping and potential terms would have to be introduced into the symmetrized Hamiltonian, or one would have to use complex parameters determining the factor ordering.

$$-(1+e^{i\theta})R\ln^2 R\frac{d}{dR}\frac{R^{-b}}{\ln R}\psi\Big|_{R\to 0} = i(1-e^{i\theta})R\frac{d}{dR}R^{-b}\psi\Big|_{R\to 0} \tag{20}$$

for $a=-1$. The extensions are parametrized by an angle $\theta\in[0,2\pi)$.

One might notice that in (19) and (20) the powers of R do not match up, and one might hence suspect that the dimensions could be wrong. In the construction of self-adjoint extensions for singular operators one has to insert a dimensionful parameter into the boundary condition we have given above in order to make the dimensions match. Usually one chooses for this parameter a relevant scale for the problem at hand, see e.g., [41]. The only meaningful scale in our case is the Planck scale, which in the units chosen here is equal to one, and as such is not visible in (19) and (20). We could insert an arbitrary dimensionful parameter into the above expressions, but it would not influence the results below in any meaningful way.

The next step is to compute the spectrum of the Hamiltonian and obtain the generalized eigenbasis. We will refrain from mathematical rigor and take the usual shortcut of enforcing the boundary conditions of the self-adjoint extensions, (19) and (20), where applicable, on our stationary modes ϕ^1_E, ϕ^2_E, and ϕ^2_{-E}. The second negative energy mode ϕ^1_{-E} is discarded because it is not square integrable and can also not be treated by Gel'fand triples because it is exponentially increasing.

Let us first consider $|1+a|<3$, and start with ϕ^2_{-E}, see (13), the last stationary mode remaining in the Hilbert space. For the case $a\neq -1$,

$$\begin{aligned} &R^{1\mp|1+a|}\frac{d}{dR}R^{-\frac{1}{2}(1+a\mp|1+a|+2b)}\phi^2_{-E} \\ &\quad= -\sqrt{2E}R^{\frac{1}{2}(3\mp|1+a|)}K_{1\mp\frac{1}{3}|1+a|}\left(\frac{2}{3}\sqrt{2E}R^{\frac{3}{2}}\right) \\ &\quad\overset{R\to 0}{\sim} -\frac{3}{2}\Gamma\left(1\mp\frac{1}{3}|1+a|\right)\left(\frac{1}{3}\sqrt{2E}\right)^{\pm\frac{1}{3}|1+a|}. \end{aligned}$$

Inserting these expressions into (19) shows that for $\theta\in(\pi,2\pi)$ the stationary mode ϕ^2_{-E} evolves unitarily under the time-dependent Schrödinger equation at one specific energy determined by

$$\left(\frac{1}{3}\sqrt{2E}\right)^{\frac{2}{3}|1+a|} = -\tan\frac{\theta}{2}\,\frac{\Gamma(1+\frac{1}{3}|1+a|)}{\Gamma(1-\frac{1}{3}|1+a|)}.$$

This energy corresponds to a bound state. The condition can only be fulfilled for values of θ with $\tan\frac{\theta}{2}<0$. For other values of θ, (19) is violated for each energy. It remains to check the case $a=-1$, for which one finds a similar restriction:

$$\ln\left(\frac{2}{3}\sqrt{2E}\right) = \frac{3}{2}\tan\frac{\theta}{2}.$$

In contrast to $a\neq -1$, this holds for all $\theta\neq\pi$.

Now we turn to the positive energy modes. Since in contrast to ϕ^2_{-E} they are not square integrable, we will not interpret them as bound states, but identify them with the continuous part of the spectrum, $E\in\mathbb{R}^+$. As explained in detail in Appendix B, only the linear combination

$$\begin{aligned}\phi_E(R) = &-\tan\frac{\theta}{2}\,\frac{\Gamma(1+\frac{1}{3}|1+a|)}{\Gamma(1-\frac{1}{3}|1+a|)}\left(\frac{1}{3}\sqrt{2E}\right)^{-\frac{2}{3}|1+a|}\phi^1_E \\ &-\cos\left(\frac{\pi}{3}|1+a|\right)\phi^1_E+\sin\left(\frac{\pi}{3}|1+a|\right)\phi^2_E \end{aligned}\tag{21}$$

for $a\neq -1$ and

$$\phi_E(R) = \left(\frac{3}{\pi}\tan\frac{\theta}{2}-\frac{2}{\pi}\ln\left(\frac{2}{3}\sqrt{2E}\right)\right)\phi^1_E+\phi^2_E \tag{22}$$

for $a=-1$ fulfill (19) and (20), respectively, for all positive energies. We will consider only ϕ_E in the construction of wave packets, which we will undertake below. Note that for $\theta=\pi$, where $\tan\frac{\theta}{2}$ diverges, (21) and (22) are not valid and have to be substituted for ϕ^1_E on its own.

Aside from $\theta=\pi$ there is also the distinguished value $\theta=0$, for which the mode (21) takes the particularly simple form

$$\begin{aligned}&\cos\left(\frac{\pi}{3}|1+a|\right)\phi^1_E-\sin\left(\frac{\pi}{3}|1+a|\right)\phi^2_E \\ &\quad= R^{\frac{1}{2}(1+a+2b)}J_{-\frac{1}{3}|1+a|}\left(\frac{2}{3}\sqrt{2E}R^{\frac{3}{2}}\right).\end{aligned}\tag{23}$$

We note that one cannot construct a mode of this type that fulfills (19) and (20) for all negative energies, since there we only have ϕ^2_{-E} at our disposal. Hence, the negative half line is not part of the spectrum of the Hamiltonian, and negative energies are restricted to those of stationary bound states.

Finally we want to mention that for $|1+a|\geq 3$, where the Hamiltonian is essentially self-adjoint, there are no bound states, since ϕ^2_{-E} is not square integrable, and ϕ^1_E is the only stationary mode that is available for constructing wave packets, as we will see in the next subsection.

Along the same lines we will see that ϕ^2_{-E} also has to be ruled out for constructing wave packets for $|1+a|\geq 3$, such that for all factor orderings only positive energy wave packets exist.

C. Wave packets and singularity avoidance

We want to construct wave packets by superposing stationary modes of different energies. Without actually

calculating the integral involved in this procedure, we are able to estimate the behavior of these wave packets towards the singularity from the behavior of the stationary modes they are constructed from. This is possible because the stationary modes are well described by power series with terms of the form $\sqrt{E}^{\alpha} \cdot R^{\beta}$ for $R \to 0$ [42]. By integrating this series term by term and assuming that the function A below (the wave packet in energy space) is well behaved, it follows that the leading term in the full wave packet behaves like the leading term of the stationary mode,

$$\Psi(R,\tau) = \int_0^\infty d\sqrt{E}\, \phi_E(R) e^{iE\tau} A(\sqrt{E}) \tag{24}$$

$$\sim R^{\beta} \int_0^\infty d\sqrt{E}\, \sqrt{E}^{\alpha} e^{iE\tau} A(\sqrt{E}). \tag{25}$$

Note that the Bessel function $Y_\nu(z)$ can only be expressed by a power series as required above when its order ν is not an integer, which means that we have to exclude these cases. The same holds for $K_\nu(z)$, but this is only marginally relevant here.

We first consider ϕ_E^1. For $z \to 0$, $J_\nu(z)$ behaves according to

$$J_\nu(z) \sim \frac{1}{\Gamma(\nu+1)} \left(\frac{z}{2}\right)^{\nu}, \quad \nu \neq -1, -2, -3, \ldots, \tag{26}$$

and hence ϕ_E^1 approaches the singularity as

$$R^{\frac{1}{2}(1-a-2b)} \phi_E^1 \sim \frac{\left(\frac{1}{3}\sqrt{2E}\right)^{\frac{1}{3}|1+a|}}{\Gamma(1+\frac{1}{3}|1+a|)} R^{1+\frac{1}{2}|1+a|} \to 0. \tag{27}$$

Not only is ϕ_E^1 square integrable near the singularity, the probability distribution $R^{1-a-2b}|\Psi|^2$ for the radius R, the norm squared of (27), even vanishes at $R \to 0$. This behavior then also holds for any wave packet constructed from ϕ_E^1: For any such wave packet, regardless of the factor ordering and the specific function A, *the probability for the outermost dust shell to be in the classically singular configuration $R = 0$ is zero*. In this sense these wave packets avoid the singularity. This criterion for singularity avoidance is close to the DeWitt criterion, cf. [8].

As we have seen in the last subsection, we can only use ϕ_E^1 on its own as a basis for wave packets when $\theta = \pi$, or, as we will see shortly, when $|1+a| \geq 3$. For other self-adjoint extensions and factor orderings, we have to consider the linear combination (21), which also includes ϕ_E^2. Apart from a prefactor, $Y_\nu(z)$ behaves for $z \to 0$ as $K_\nu(z)$ does, which means that ϕ_E^2 behaves according to (18) when approaching the singularity. It thus follows that ϕ_E^2 (and ϕ_{-E}^2) must be excluded for the construction of wave packets for $|1+a| \geq 3$, because those wave packets would not be square integrable when approaching the singularity; so only ϕ_E^1 remains. Similarly, for ϕ_E^2 singularity avoidance occurs along the same lines as for ϕ_E^1 only when $|1+a| < 2$.

We can see that the singularity is always avoided for factor orderings where $|1+a| \geq 3$ or $|1+a| < 2$, with the possible exception of $\frac{1}{3}|1+a| \in \mathbb{N}$. We want to emphasize again that this avoidance holds independently of the chosen self-adjoint extension and the specific wave packet. Notably, both the naive ($a = b = 0$) and the Laplace-Beltrami factor ordering ($b = 0$, $a = \frac{1}{2}$) fall into this category of guaranteed singularity avoidance. The case $\theta = \pi$ should also be highlighted, because there singularity avoidance occurs independently of the factor ordering.

For the cases where we do not have a guaranteed singularity avoidance, we have instead the guarantee that the probability distribution for R *does* have support at the singularity. Thus, depending on the factor ordering and self-adjoint extension, either the singularity does play a role or it does not; we cannot influence this by our choice of wave packet. It should be noted that the remaining stationary mode (13) also does not avoid the singularity for $2 \leq |1+a| < 3$. Since in addition to being stationary it has a negative energy, which moreover depends heavily on the factor ordering and the choice of self-adjoint extension, it can safely be excluded when discussing gravitational collapse.

To summarize, we see that singularity avoidance is not only possible but even guaranteed for a wide class of the quantum models considered here, and shows a remarkable robustness under many of the quantization ambiguities. No artificial fine-tuning is required to achieve this result.

D. A unitarily evolving wave packet

To find out how exactly singularity avoidance is facilitated, we want to construct a positive energy wave packet. We choose the self-adjoint extension $\theta = \pi$ in order to use ϕ_E^1 for its construction for all factor orderings.

Useful for the construction of nonstationary modes from ϕ_E^1 is the closure equation [see e.g., [43], Eq. (11.59)]

$$\int_0^\infty dx\, x\, J_\nu(ax) J_\nu(bx) = \frac{\delta(a-b)}{a}, \quad \text{for } \nu > -\frac{1}{2}.$$

The Bessel functions form an orthogonal set under the scalar product used above. This property also holds in our Hilbert space for the mode ϕ_E^1,

$$\int_0^\infty dR\, R^{1-a-2b} \phi_E^1(R) \phi_{\tilde{E}}^1(R) = \frac{3}{4\sqrt{E}} \delta\left(\sqrt{E} - \sqrt{\tilde{E}}\right).$$

It is more practical to deal with an orthonormal set of modes, hence we rescale ϕ_E^1 as

$$\tilde{\phi}^{\frac{1}{2}}_E(R) = \frac{2}{\sqrt{3}} E^{\frac{1}{4}} R^{\frac{1}{2}(1+a+2b)} J_{\frac{1}{3}|1+a|}\left(\frac{2}{3}\sqrt{2E}R^{\frac{3}{2}}\right).$$

Our ansatz for constructing wave packets from stationary solutions reads, as noted before,

$$\Psi(R,\tau) = \int_0^\infty d\sqrt{E}\,\tilde{\phi}_E(R) e^{iE\tau} A(\sqrt{E}). \tag{28}$$

For the function $A(\sqrt{E})$ we choose a Poisson-like distribution similar to the one used in [4] for collapsing null shells,

$$A(\sqrt{E}) = \frac{\sqrt{2}\lambda^{\frac{1}{2}(\kappa+1)}}{\sqrt{\Gamma(\kappa+1)}} \sqrt{E}^{\kappa+\frac{1}{2}} e^{-\frac{\lambda}{2}\sqrt{E}^2},$$

where $\kappa \geq 0$ and $\lambda > 0$ are real parameters. We note that κ is dimensionless and λ has the dimension of length. The function is normalized,

$$\int_0^\infty d\sqrt{E}\, A^2(\sqrt{E}) = 1.$$

The mean (square root of the) energy and its width are

$$\overline{\sqrt{E}} = \int_0^\infty d\sqrt{E}\sqrt{E} A^2(\sqrt{E}) = \frac{1}{\sqrt{\lambda}} \frac{\Gamma(\kappa+\frac{3}{2})}{\Gamma(\kappa+1)},$$
$$\Delta\sqrt{E} = \frac{1}{\sqrt{\lambda}} \sqrt{\kappa+1-\frac{\Gamma^2(\kappa+\frac{3}{2})}{\Gamma^2(\kappa+1)}}.$$

Because we have chosen $A(\sqrt{E})$ appropriately, there is a closed form for $\Psi(R,\tau)$ in terms of Kummer's confluent hypergeometric function ${}_1F_1(a;b;z)$ [see e.g., [44], Eq. (1) in 6.631],

$$\Psi(R,\tau) = \sqrt{3}\left(\frac{\sqrt{2}}{3}\right)^{\frac{1}{3}|1+a|+1} \frac{\Gamma(\frac{1}{6}|1+a|+\frac{\kappa}{2}+1)}{\sqrt{\Gamma(\kappa+1)}\Gamma(\frac{1}{3}|1+a|+1)} \times R^{\frac{1}{2}(1+a+|1+a|+2b)} \frac{\lambda^{\frac{1}{2}(\kappa+1)}}{(\frac{\lambda}{2}-i\tau)^{\frac{1}{6}|1+a|+\frac{\kappa}{2}+1}} \times {}_1F_1\left(\frac{1}{6}|1+a|+\frac{\kappa}{2}+1;\frac{1}{3}|1+a|+1;-\frac{2R^3}{9(\frac{\lambda}{2}-i\tau)}\right). \tag{29}$$

The behavior of the wave packet can be seen in Fig. 1. It first follows the infalling classical trajectory up to some minimal R and then makes a transition to the outgoing classical trajectory: the outermost shell of a collapsing LTB model bounces before reaching the singularity. Depending on the parameters of the wave packet, the shell can even fall significantly far below the apparent horizon until it switches from collapse to expansion. It should be emphasized that this transition is classically forbidden and can be interpreted as tunneling from a collapsing to an expanding configuration, or, in a heuristic picture, from BH to WH.

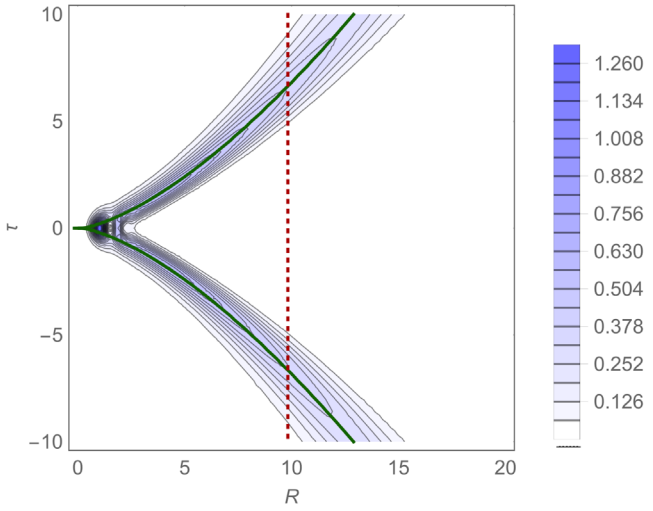

(a) $\lambda = 2.2$ and $\kappa = 9.8$

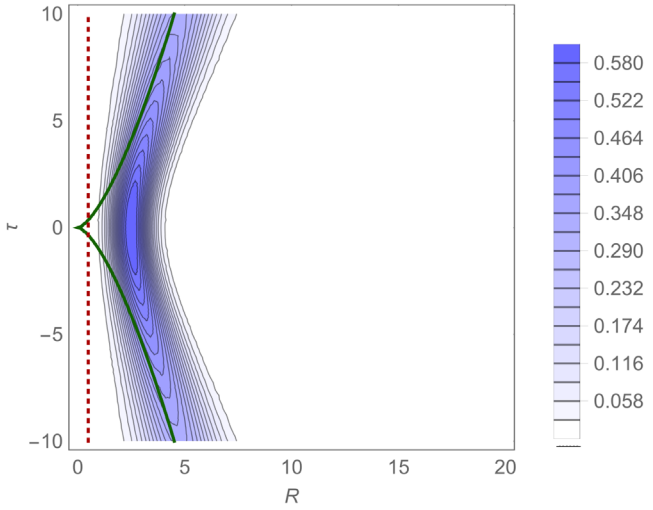

(b) $\lambda = 8.08$ and $\kappa = 0.96$

FIG. 1. Probability amplitude for R as given by $R^{1-a-2b}|\Psi(R,\tau)|^2$, compared to the classical trajectories $R_{cl} = (\mp\frac{3}{2}\sqrt{2}\tau)^{\frac{2}{3}}\sqrt[3]{E^2} = (\mp\frac{3}{2}\sqrt{\frac{2}{\lambda}}\tau)^{\frac{2}{3}}\frac{\Gamma(\kappa+\frac{4}{3})}{\Gamma(\kappa+1)}$ (full green line) and the exterior apparent horizon $R_{AH} = 2\bar{E} = 2\frac{\kappa+1}{\lambda}$ (dotted red line), with $a = 2$ and $b = 1$, and different λ and κ.

So far this model shares its main features with the quantum collapse of a null shell [3,4], but in one aspect it differs: the wave packet describing the null shell shows little dispersion, while in our case the wave packet increases in width when proceeding away from the singularity. This is in contrast to minisuperspace models in quantum cosmology, where dispersion near the singularity was interpreted as a mechanism for singularity avoidance; see, for example, [8,45].

We note that the probability distribution for the radius R shows oscillatory behavior near the $\tau = 0$ line for high energies, see Fig. 1(a). This interferencelike pattern emerges because in this region the part of the wave packet centered around the classical collapsing trajectory is superposed on the wave packet around the expanding trajectory. In this sense one could also state that the singularity avoidance results from destructive interference between two separate wave packets corresponding to BH and WH, respectively.

We also note that the general form of Fig. 1 does not seem to change with the factor ordering; the bouncing behavior is always present. In fact, the parameter b completely cancels out in the probability distribution $R^{1-a-2b}|\Psi(R,\tau)|^2$. The details of this distribution depend, however, on a, such as the position of its peak at $\tau = 0$.

One can demonstrate that this bouncing behavior shows a certain robustness also under other details of the quantization: for $\theta = 0$, one can choose the mode (23) for the construction of wave packets as long as $|1+a| < 3$. Due to the similarity of this mode to ϕ^1_E one can extend our wave packet to this case by simply introducing a few negative signs at places where the order of the Bessel function enters. Checking the corresponding plots shows that this wave packet still bounces. For some factor orderings this may even happen out from a singular configuration. We see that this behavior is not only robust under changes of the factor ordering, but also under different choices of self-adjoint extension.

To discuss the bouncing behavior more rigorously we want to calculate, for example, the expectation value of the radius R of the outermost shell. In its current form, our wave packet is too complex to perform concrete calculations, but fortunately it can be significantly simplified. We set $\kappa = \frac{1}{3}|1+a|$ and use the identity ${}_1F_1(a;a;z) = e^z$ [[42], Eq. (13.6.1)] to arrive at the wave packet

$$\tilde{\Psi}(R,\tau) = \sqrt{3}\frac{R^{\frac{1}{2}(1+a+|1+a|+2b)}}{\sqrt{\Gamma(\frac{1}{3}|1+a|+1)}}\left(\frac{\frac{\sqrt{2\lambda}}{3}}{\frac{\lambda}{2}-i\tau}\right)^{\frac{1}{3}|1+a|+1} \times \exp\left(-\frac{2R^3}{9(\frac{\lambda}{2}-i\tau)}\right). \tag{30}$$

In quantum cosmology, a similar trick was used in [46].

As we will see below, by this simplification we have gained the ability to compute quantities such as $\bar{R}(\tau)$ analytically, but of course this comes at a cost. We cannot independently adjust $\sqrt{E}$ and $\Delta\sqrt{E}$ anymore, since both are now proportional to $1/\sqrt{\lambda}$. The relative width in energy of the wave packet is now fixed by the factor ordering to

$$\frac{\Delta\sqrt{E}}{\sqrt{E}} = \sqrt{\frac{\Gamma(\frac{1}{3}|1+a|+2)\Gamma(\frac{1}{3}|1+a|+1)}{\Gamma^2(\frac{1}{3}|1+a|+\frac{3}{2})}-1} \leq \left.\frac{\Delta\sqrt{E}}{\sqrt{E}}\right|_{a=-1} \approx 0.53.$$

We see that this wave packet can be rather broadly peaked on its mean energy, depending on a. To decrease its width significantly, one has to consider factor orderings far beyond the usual ones: $\frac{\Delta\sqrt{E}}{\sqrt{E}} \approx 0.2$ for $a = 14$, and $\frac{\Delta\sqrt{E}}{\sqrt{E}} \approx 0.1$ for $a = 71$. As we have stated above, the bouncing behavior of (29) is still present for high values of $|1+a|$, hence it seems reasonable that results for a $\tilde{\Psi}$ with some well-defined energy (and therefore very high or low a) will also be applicable similarly to more reasonable values of a when considering wave packets of the form (29) and narrow in energy.

For (30) we can now compute $\bar{R}$ and ΔR,

$$\bar{R} = \left(\frac{9\lambda}{8}+\frac{9\tau^2}{2\lambda}\right)^{\frac{1}{3}}\frac{\Gamma(\frac{1}{3}|1+a|+\frac{4}{3})}{\Gamma(\frac{1}{3}|1+a|+1)}, \tag{31}$$

$$\Delta R = \bar{R}\sqrt{\frac{\Gamma(\frac{1}{3}|1+a|+\frac{5}{3})\Gamma(\frac{1}{3}|1+a|+1)}{\Gamma^2(\frac{1}{3}|1+a|+\frac{4}{3})}-1} \tag{32}$$

$$\leq \Delta R|_{a=-1} \approx 0.37\cdot\bar{R}. \tag{33}$$

As expected, $\bar{R}(\tau)$ is symmetric in τ and has a global minimum at $\tau = 0$, the minimal radius scaling inversely with the energy for fixed relative width $\frac{\Delta\sqrt{E}}{\sqrt{E}}$,

$$R_0 := \bar{R}(0) = \left(\frac{9}{8}\lambda\right)^{\frac{1}{3}}\frac{\Gamma(\frac{1}{3}|1+a|+\frac{4}{3})}{\Gamma(\frac{1}{3}|1+a|+1)} \propto \frac{1}{\bar{E}^{\frac{1}{3}}}. \tag{34}$$

That the dependence of R_0 on the energy carries over to (29) can be checked analytically. One finds that

$$\bar{R}(\tau=0) = \lambda^{\frac{1}{3}}g(a,\kappa).$$

The function $g(a,\kappa)$ is rather complicated and can be found in Appendix C. When keeping the relative width (and hence κ) and the factor ordering constant, this expression is proportional to $\bar{E}^{-\frac{1}{3}}$, as for the simplified wave packet. Furthermore, it seems that $\bar{R}(\tau=0)$ increases with decreasing relative width in energy and with increasing $|1+a|$, but a more rigorous analysis is prevented by the complicated form of $g(a,\kappa)$.

This result is in contradiction to [9], in which by heuristic arguments $R_0 \propto E^n$, with $n = \frac{1}{3}$ or $n = 1$, was obtained. Our considerations predict (in the language of [9]) a Planck star, meaning a temporary compact remnant of gravitational collapse, with sub-Planckian size. For example, for a dust cloud with solar mass (taking $\kappa = 24$, meaning $\frac{\Delta\sqrt{E}}{\sqrt{E}} \approx 0.1$ and $a = 1$) we get $\bar{R}(\tau=0) \approx 10^{-13} l_{\mathrm{P}} \approx 10^{-48}$ m.

One has to be careful when interpreting this result. Recall that we only consider the outermost dust shell, but during the bounce the order of the shells might get reversed, as suggested by the inverse scaling of R_0 with E. Remarkably,

in that case the size of the compact object is not necessarily connected to the total mass of the initial dust cloud, but rather to its structure near the center. The minimal size of the dust cloud, potentially equal to the minimal radius of the innermost dust shell, might then be considerably higher. For example, with the Planck mass as $\bar{E}$ and the other parameters kept the same, R_0 is of the same order of magnitude as the Planck length. We will present more details on various aspects of this remnant in Sec. IV and return now to the simplified wave packet and the corresponding expectation value $\bar{R}$.

We can show analytically that $\bar{R}(\tau)$ is approximated very well by classical trajectories when far away from the singularity, as illustrated in Fig. 1. For $\tau^2 \gg \lambda^2$,

$$\bar{R}(\tau) \approx \left(\frac{3}{2}\sqrt{2}|\tau|\right)^{\frac{2}{3}} \frac{\Gamma(\frac{1}{3}|1+a|+\frac{4}{3})}{\lambda^{\frac{1}{3}}\Gamma(\frac{1}{3}|1+a|+1)} = \left(\frac{3}{2}\sqrt{2}|\tau|\right)^{\frac{2}{3}} \sqrt[3]{E^2}. \tag{35}$$

It is straightforward to see that this is a solution to (2) for $R(\tau=0)=0$.

IV. QUANTUM CORRECTED SPACETIME FOR DUST COLLAPSE

Based on the dynamics of the wave packet discussed in the last section, one can construct a quantum corrected spacetime describing bouncing dust collapse. In this section, we will discuss some aspects of this spacetime.

We take the marginally bound LTB metric,

$$ds^2 = -d\tau^2 + (\partial_\rho R)^2 d\rho^2 + R^2 d\Omega^2,$$

and use the quantum dynamics of the outermost dust shell to fix the function $R(\tau,\rho)$. We will focus our discussion on heavy dust clouds and on corresponding wave packets with a narrow width, such that they follow the classical trajectories far behind the horizon.

Depending on what we want to discuss it suffices to simply set $R(\rho \to \rho_o) = \bar{R}$, such that the trajectory of the outermost shell matches the expectation value of the corresponding wave packet. Thereby we leave the evolution of the other shells completely open, except that they be contained in the outermost shell at least far away from the singularity. This is the case for our investigation of the horizon and its lifetime. To compute the effective pressures arising near the bounce of the quantum corrected spacetime, we have to make use of the fact that our Hamiltonian gives the correct dynamics for every single shell, and generalize $\bar{R}$ to $\bar{R}(\rho)$.

We will see that at some points further corrections must be made in order to account for some inconsistencies of this spacetime. Hence we will recall the quantum theory in the background and evoke some of its properties other than the corrected dust trajectories where necessary.

A. Horizon

We have already mentioned that in classical dust clouds apparent horizons appear where the condition $F(\rho) = R(\tau,\rho)$ is fulfilled. Attaching a Schwarzschild exterior to the classical LTB model, an apparent horizon can pass to this exterior from the outermost shell when the radius of that shell becomes smaller than $2E_{\mathrm{ADM}}$. Hence, it is the outermost dust shell that determines the position of this horizon via the mass contained in it, and whether the horizon is future or past via the sign of its velocity. We will see in the following that in our quantum corrected spacetime the exterior horizon's behavior is not quite as easily determined.

First we want to determine the position of the horizon. Calculating the Misner-Sharp mass for the corrected trajectory $R(\tau) = (R_0^3 + \frac{9E}{2}\tau^2)^{\frac{1}{3}}$, one finds

$$M_{\mathrm{MS}} = E\frac{R^3 - R_0^3}{R^3},$$

see (31) and (34). We have seen previously that for heavy dust clouds $R_0 \ll 2E$, meaning $R_{\mathrm{AH}} = 2E$ is still approximately the position of the apparent horizon in question for early and late times, since $2E \approx 2M_{\mathrm{MS}}(R \gg R_0)$.

Close to the bounce the situation is more complicated. Because M_{MS} changes in time, one cannot simply match the dust cloud to a Schwarzschild solution at the outermost shell. As we will see in Sec. IV C, effective pressures occur in our quantum corrected spacetime, which further prevent the matching to an exterior region [47]. Taking the exterior apparent horizon to be at $R_{\mathrm{AH}} = 2M_{\mathrm{MS}}$, we can see that when approaching the bounce the apparent horizon shrinks and even disappears for $R = R_0$, which means that it will vanish back into the dust cloud for some time during the bounce. This is in agreement with other propositions for the behavior of the horizon in similar models [20].

In the following, we will assume that an exterior horizon is present at $R = 2E$ as long as the outermost shell is inside this radius, since this introduces the least radical modification into the corrected spacetime. This leaves us to explain the transition of the horizon from BH to WH.

Recall that whether the horizon in question is future or past is determined by the sign of $\dot{R}$. For the BH it is negative, while it is positive for the WH. If we limit ourselves to just the quantum corrected spacetime, the horizon will of course be either future or past, with an instantaneous transition when the shell turns around. To smooth out this process we can invoke the quantum model and allow the horizon to be in a superposition, as was done in [3].

Classically, the momentum $P = -2R\dot{R}$ always has the opposite sign to $\dot{R}$, meaning the nature of the horizon can be

determined with the help of the operator $\hat{P}$. Unfortunately, as is well known for the momentum operator on the half line, it cannot be made self-adjoint, meaning $\hat{P}$ is not technically an observable. Nevertheless, for the calculation of an expectation value a symmetrized version of $\hat{P}$ is sufficient. The operator

$$\hat{\mathsf{P}} = -iR^{-\frac{1}{2}(1-a-2b)}\frac{\partial}{\partial R}R^{\frac{1}{2}(1-a-2b)}$$

fits our purposes. Now we can calculate the expectation value of $\hat{\mathsf{P}}$ with respect to the simplified wave packet (30),

$$\begin{aligned}\bar{\mathsf{P}} &= -i\left(1+\frac{1}{2}|1+a|\right)\overline{R^{-1}} + i\frac{2}{3(\frac{\lambda}{2}-i\tau)}\overline{R^2}\\ &= -3\tau\left(\frac{9\lambda}{8}+\frac{9\tau^2}{2\lambda}\right)^{-\frac{1}{3}}\frac{\Gamma(\frac{1}{3}|1+a|+\frac{5}{3})}{\lambda\Gamma(\frac{1}{3}|1+a|+1)} \propto -\tau.\end{aligned}$$

This shows the behavior one would expect: before the bounce we have $\mathrm{sgn}\bar{\mathsf{P}} > 0$ and hence a BH horizon, and afterwards with $\mathrm{sgn}\bar{\mathsf{P}} < 0$ a WH horizon. We can make an educated guess concerning the transition in between by normalizing $\bar{\mathsf{P}}$ by the condition that at $\tau \to -\infty$ the wave packet was in a pure BH state, to which we assign the value 1 (and correspondingly to a WH -1), leading to

$$\bar{\mathsf{p}} = \frac{\bar{\mathsf{P}}}{\bar{\mathsf{P}}_{\tau\to-\infty}} = -\mathrm{sgn}\tau\left(\frac{\tau^2}{\frac{\lambda^2}{4}+\tau^2}\right)^{\frac{1}{3}}. \tag{36}$$

$\bar{\mathsf{P}}_{\tau\to-\infty} \propto (\frac{2}{9}\lambda|\tau|)^{\frac{1}{3}}$ is the asymptotic behavior of $\bar{\mathsf{P}}$ at very early times, for the normalization extended to all τ. Taking $\bar{\mathsf{p}}$ as a measure of "black hole-ness," we see that the transition from BH to WH is instantaneous for $\lambda \to 0$, and smoothed out for higher values of the parameter. Note that the minimal radius (34) scales with a positive power of λ. It follows that the closer the wave packet comes to the singularity, the more rapid is the transition of the horizon.

Taking into account that during the bounce the order of the shells might get "scrambled" such that the outermost shell need not stay outermost, it would be appropriate to alter the exact form of the horizon transition to reflect the behavior of the shell that actually has the largest radius at a given τ. We would then expect a further smoothing of the transition.

B. Lifetime

The lifetime of the exterior horizon is of great interest as a consistency check of our model. It should be long enough such that the bouncing collapse at least resembles a BH; otherwise, this scenario would be excluded by astrophysical observations.

In order to discuss this lifetime we introduce two observers into the spacetime, one at a fixed physical radius R_{obs} and the other comoving with the dust cloud. These two observers will meet twice, first during the collapse and again during the reexpansion. The time difference between these two events for the comoving observer is then given by

$$\Delta\tau = \tau_+ - \tau_- = \sqrt{\frac{8R_{\mathrm{obs}}^3}{9}\frac{\lambda\Gamma^3(\frac{1}{3}|1+a|+1)}{\Gamma^3(\frac{1}{3}|1+a|+\frac{4}{3})} - \lambda^2},$$

where $\tau_\pm$ is defined by $R_{\mathrm{obs}} = \bar{R}(\tau_\pm)$. For a heavy cloud and a fixed relative width in energy, λ has to be small; we can thus neglect the second term under the square root and find

$$\begin{aligned}\Delta\tau &= \sqrt{\frac{8R_{\mathrm{obs}}^3}{9}}\left(\frac{\lambda^{\frac{1}{3}}\Gamma(\frac{1}{3}|1+a|+1)}{\Gamma(\frac{1}{3}|1+a|+\frac{4}{3})}\right)^{\frac{3}{2}}\\ &= \sqrt{\frac{8R_{\mathrm{obs}}^3}{9\overline{E^{\frac{1}{3}}}^3}} \le \sqrt{\frac{8R_{\mathrm{obs}}^3}{9\bar{E}}}.\end{aligned}$$

The last step follows from Hölder's inequality, $\overline{X^q} \le \overline{X^p}^{\frac{q}{p}}$ for $0 < q < p$. For narrow wave packets one would expect the last two terms to be nearly equal. This result is equal to twice the free fall time of the outermost shell from an initial radius R_{obs} down to $R = 0$.

The lifetime of the grey hole can then be taken to be $\Delta\tau$ with $R_{\mathrm{obs}} = \overline{R_{\mathrm{AH}}}$,

$$\Delta\tau_{\mathrm{GH}} \approx \frac{8}{3}\bar{E}.$$

The lifetime from the point of view of the comoving observer scales linearly with the dust cloud's mass, an unsurprising result given how closely $\bar{R}$ sticks to the classical trajectories. More interesting for comparison with observations is the timescale experienced by the other, external observer.

It is at this point that we run into a problem: The exterior of our bouncing dust cloud at least at early and late times can be described via a Schwarzschild black hole or, more precisely, appropriate patches of the Kruskal spacetime. In terms of Schwarzschild Killing time, which a stationary observer very far from the dust cloud approximately experiences, crossing the apparent horizon (which for a heavy dust cloud happens at sufficiently early and late times) takes infinitely long. This prediction seems paradoxical: The comoving observer returns in finite time to his exterior counterpart, for whom an infinite amount of time has passed. The outside observer would see his more adventurous friend as being stuck when approaching the apparent horizon.

It appears that further modification of the quantum corrected spacetime is necessary, as was also argued in [16,48], and in a different context in [49]. Unfortunately, our model is formulated in terms of dust proper time, and

we have cut off the exterior geometry. Hence, calculating the lifetime as seen from the exterior observer would entail transforming to Schwarzschild Killing time, which is ill-defined in the quantum model, since this transformation depends on R and on the energy E. Attaching an exterior to the dust cloud is also problematic, as we have discussed in the last section; it is also ambiguous because the time delay between horizon crossings is an open parameter [16].

We will instead follow a different approach by incorporating another physical mechanism into the quantum corrected spacetime picture: transitions between dynamically distinct "states" of the dust cloud, sticking closely to the picture of BHWH tunneling as employed in [18,19]. There, the lifetime of a bouncing null dust shell was computed in a way which in the following we will adapt to our model.

We differentiate between three states of the dust cloud: collapsing while being at least partially outside its horizon; being completely inside the horizon (referred to below as the grey hole); and expanding outside of its horizon.

We then consider the following setup. The cloud, characterized by its outermost shell, behaves semiclassically up until close to the horizon, in accordance with our previous results. Due to the aforementioned gravitational time dilation, quantum-gravitational effects have a chance to accumulate. At this point, the dust cloud will inevitably experience a transition to one of the other states listed above. Furthermore, motivated by results for the BHWH tunneling timescale [5,17,19], we assume that the transition itself takes a relatively short amount of time, roughly proportional to the mass of the dust cloud.

This accumulation, or pileup, of quantum effects when approaching the horizon was first proposed by Haggard and Rovelli in [16]. We want to note that this mechanism cannot straightforwardly be applied as an explanation for the transition of the horizon, as there one cannot take the distinguished notion of time to be Schwarzschild Killing time.

To determine the lifetime we need to compute the relevant transition probabilities. We will take these probabilities to be determined by our quantum model,

$$W(\tau_-,\tau_+) = \left|\int_0^\infty dR\, R^{1-a-2b}\tilde{\Psi}^*(R,\tau_-)\tilde{\Psi}(R,\tau_+)\right|^2 = \left(\frac{\lambda^2}{\lambda^2+(\tau_+-\tau_-)^2}\right)^{\frac{1}{3}|1+a|+1}.$$

The three states can then be characterized by ranges in proper time: $\tau < -\tau_{\mathrm{AH}}$ for collapse (C), $-\tau_{\mathrm{AH}} < \tau < \tau_{\mathrm{AH}}$ for the grey hole (GH), and $\tau_{\mathrm{AH}} < \tau$ for expansion (E). $\pm\tau_{\mathrm{AH}}$ with $\tau_{\mathrm{AH}} > 0$ are the proper times at which the outermost shell reaches the apparent horizon, $\bar{R}(\pm\tau_{\mathrm{AH}}) = 2\bar{E}$.

Let us now follow the dust cloud from the collapsing to the expanding state. First, the outermost shell approaches the apparent horizon from the outside and will eventually make a transition either to the grey hole or to the expanding state. Which case is more likely?

To answer this question, let us consider the transition probabilities:

$$\frac{P_{\mathrm{C}\to\mathrm{E}}}{P_{\mathrm{C}\to\mathrm{GH}}} = \frac{\int_{-\infty}^{-\tau_{\mathrm{AH}}} d\tau_- \int_{\tau_{\mathrm{AH}}}^{\infty} d\tau_+ W(\tau_-,\tau_+)}{\int_{-\infty}^{-\tau_{\mathrm{AH}}} d\tau_- \int_{-\tau_{\mathrm{AH}}}^{\tau_{\mathrm{AH}}} d\tau_+ W(\tau_-,\tau_+)} \approx \frac{(2\frac{\tau_{\mathrm{AH}}}{\lambda})^{-\frac{2}{3}|1+a|}}{\frac{2}{3}|1+a|+1}.$$

This is an approximation for high energies of the full expression, which can be found in Appendix D. We have used that $\tau_{\mathrm{AH}}/\lambda$ roughly scales with $\bar{E}^2$. It follows that for high energies (and nonmaximal relative widths of the wave packet, $a \neq -1$) the transition to the grey hole state dominates. As a result we will focus on this transition.

We will now define the lifetime as the time it takes for the dust cloud to make a transition from grey hole to the expanding state. Once in this state, the outermost shell will expand away from the apparent horizon and will not get the chance to make a transition to a different state again. It will stay outside its horizon, and the grey hole is gone. To determine this lifetime we follow [19], where a BH lifetime was computed using a picture of BHWH tunneling, and draw an analogy to an alpha particle tunneling out of a nucleus. A simple model for this process is the following: the particle travels across the nucleus and after a time Δt hits a potential wall which it can traverse with probability p. If it fails, it will be reflected and can try again when, after the time Δt has elapsed once more, it hits a potential wall on the other side. The lifetime of the nucleus can then be estimated as $\Delta t/p$.

Taking also the previously discussed transition from collapsing to GH state into account, our picture of dust collapse from the perspective of an exterior observer seems to resemble the quantum mechanical process of "resonant tunneling," where at specific energies depending on the potential barrier metastable states can occur during scattering. Some of the different notions of tunneling time (see e.g., [50]) can also be applied to resonant tunneling (see e.g., [51]). Unfortunately, this requires knowledge of the full wave function, which we do not possess. So we return to our picture of three distinct states.

What we need to determine now is the probability for the dust cloud to evolve from grey hole to expanding state, what process replaces reflection in the analogy above, and the time it takes until the cloud is ready to try escaping again. The probability can be determined as above,

$$P_{\mathrm{GH}\to\mathrm{E}} = \frac{\int_{-\tau_{\mathrm{AH}}}^{\tau_{\mathrm{AH}}} d\tau_- \int_{\tau_{\mathrm{AH}}}^{\infty} d\tau_+ W(\tau_-,\tau_+)}{\int_{-\tau_{\mathrm{AH}}}^{\tau_{\mathrm{AH}}} d\tau_- \int_{-\infty}^{\infty} d\tau_+ W(\tau_-,\tau_+)} \tag{37}$$

$$\approx \frac{\Gamma(\frac{1}{3}|a+1|)}{4\sqrt{\pi}\Gamma(\frac{1}{3}|a+1|+\frac{1}{2})}\frac{\lambda}{\tau_{\mathrm{AH}}}. \tag{38}$$

The last line is once again an approximation for high energies. We see that the probability for the dust cloud to

escape the grey hole state is proportional to $1/\bar{E}^2$ for heavy clouds.

Note that the above only holds for $a \neq -1$. For $a = -1$, the escape probability $P_{\mathrm{GH}\to\mathrm{E}}$ behaves to leading order like $\frac{\lambda}{\tau_{\mathrm{AH}}}\ln(2\frac{\tau_{\mathrm{AH}}}{\lambda})$. This is of no further concern here since we are only interested in narrow wave packets, but serves as a warning that for the full wave packet, where the width is not related to a, this result might change for this specific class of factor orderings.

Classically the only timescale at our disposal is $\bar{E}$, and hence it seems reasonable to assume that the time between escape attempts is proportional to $\bar{E}$, as also argued in [19]. We will refrain from guessing the corresponding alternative process at this point and instead leave its discussion for future work. It might not even be relevant from the point of view of the exterior observer, because there is the possibility that whatever happens is hidden behind a horizon.

Combining our results thus gives a total lifetime proportional to $\bar{E}^3$. Other contributions are negligible in comparison: We have assumed the time for the transition itself to be of the order $\bar{E}$. Furthermore, the Killing time when approaching the horizon only diverges logarithmically, and hence the time it takes until the initial transition into the grey hole takes place is, depending on how close to the horizon this occurs, most likely appreciably smaller than $\propto \bar{E}^3$.

Our lifetime is considerably larger than earlier results that predict a lifetime linear in $\bar{E}$ [5,17]. It has since been argued that this describes only the time for the transition itself, in case this happens, and should be complemented by a timescale associated with the failure to perform a transition [19]. This is also the viewpoint we adopt here, but compared to the lifetime $\propto \bar{E}e^{\Xi\bar{E}^2}$ found in [19], our lifetime is significantly smaller. It is, in fact, comparable with the Hawking evaporation time, making Hawking radiation a significant factor for the lifetime. The explicit inclusion of it deserves further investigation. Also of the same timescale is the dispersion time of a wave packet describing a quantized extremal Reissner–Nordström black hole [52].

Our result also further corroborates the usual sentiment that the semiclassical description of quantum black holes breaks down within a timescale of $\bar{E}^3$, an idea first introduced in the discussion of Hawking evaporation and supported by the results of [52]. In our model, the exterior observer first notices the bounce when this time has elapsed after the formation of the grey hole, breaking at least the global notion of a correct classical description of the geometry far away from the singularity.

In spite of its limitations, we are confident that our simple model provides convincing arguments for a finite, but not too short lifetime for the transition from BH to WH.

C. Effective pressure

For the following discussion it is necessary to generalize our results from the outermost dust shell to the full LTB model; we thus assume

$$R(\tau,\rho) = (R_0(\rho)^3 + R_{\mathrm{cl}}(\tau,\rho)^3)^{\frac{1}{3}},$$
$$\text{with}\quad R_0(\rho) = \frac{\alpha(\rho)}{F(\rho)^{\frac{1}{3}}}, \qquad \dot{R}_{\mathrm{cl}}(\tau,\rho)^2 = \frac{F(\rho)}{R_{\mathrm{cl}}(\tau,\rho)}.$$

Here, $\alpha(\rho)$ has been heuristically introduced to describe this generalization. We leave this function open, except for the condition that when approaching $\rho \to 0$, $\alpha \propto F^{\frac{1}{3}}$ such that the minimal radius of the innermost shell does not diverge. Furthermore, α has to be chosen in such a way that for every shell the initial radius is at least as big as its minimal radius.

One should note that a special case of this class of bouncing dust collapse models was discussed in [13], motivated by a specific correction of the energy density through quantum effects; the authors of [13] considered homogeneous dust and used a specific function α.

Inserting the resulting metric into the Einstein equations, we can determine an effective energy-momentum tensor. It is diagonal, and hence we interpret its components as an effective energy density and three components of (anisotropic) pressure,

$$8\pi\epsilon = \frac{1}{R'R^2}\left(F - \frac{\alpha^3}{R^3}\right)',$$
$$8\pi p_\rho = -3\frac{\alpha^3}{R^6},$$
$$8\pi p_\theta = 8\pi p_\phi = \frac{3}{2}\frac{\alpha^3}{R^6} - \frac{3}{2}\frac{1}{R'R^2}\left(\frac{\alpha^3}{R^3}\right)'.$$

As we can see, the corrections to the energy density and the pressures build up quickly very close to the bounce because of the factors R^{-6}. To facilitate the bounce, the pressure and the correction to the energy density need to become negative enough to make gravity repulsive. Adding up all contributions gives

$$8\pi(\epsilon + p_\rho + p_\theta + p_\phi) = \frac{1}{R'R^2}\left(F - 4\frac{\alpha^3}{R^3}\right)'.$$

For simplicity we will in the following consider this expression at the time of the bounce for individual shells. After all, one would expect that the repulsion is strongest then. This gives

$$8\pi(\epsilon + p_\rho + p_\theta + p_\phi)|_{R=R_0} = -3\frac{F'}{R_0'R_0^2}. \tag{39}$$

It should be noted that in agreement with the Misner-Sharp mass, ϵ vanishes at the bounce.

The expression (39) need not necessarily be negative.[2] The shells may get scrambled, that is, their order may (perhaps partially) be reversed. Because this can only be the case for the future of a shell-crossing singularity, one has to specify how the spacetime is extended through it. We have done that already in the form of the shell trajectories $R(\tau,\rho)$ above, but have to be aware that the interpretation of some quantities changes. Most relevant here is the fact that the mass function $F(\rho)$ is still constant in time, but cannot be equal to the mass contained in the shell ρ after crossing another shell. We have to interpret F as a label attached to the shells. This restriction is then lifted after the shell crossings occur a second time, and F once again regains its former status. Furthermore, we have to consider that the coordinates do not have to retain their physical meaning during the bounce: τ is not necessarily the dust proper time, a fact which will not restrict the following considerations, whereas the fact that ρ is not monotonically increasing when going outwards will become very important.

It follows that while F' is always positive, there is no guarantee that R' will stay positive during the bounce, potentially changing the sign of the effective energy density (39). If this happens, gravity can become repulsive. How can we understand this?

To answer this question we calculate the active gravitating mass inside the shell ρ by the following integral, at first without any scrambling,

$$M(\rho,\tau) = 4\pi \int_0^\rho d\tilde{\rho}\, \sqrt{-g}\,(\epsilon + p_\rho + p_\theta + p_\phi) = \frac{F}{2} - 2\frac{\alpha^3}{R^3} \overset{R=R_0}{=} -\frac{3}{2}F.$$

As expected, gravity becomes repulsive, and also stronger by a factor of 3 as compared to the classical collapse.

We now address the case of scrambling which we restrict to the case where the order of all shells is completely reversed. Taking into account that the innermost shell is then the former outermost one with $\rho = \rho_o$, we have

$$M(\rho,\tau) = 4\pi \int_{\rho_o}^\rho d\tilde{\rho}\, \sqrt{-g}\,(\epsilon + p_\rho + p_\theta + p_\phi) = \left[-\frac{F}{2} + 2\frac{\alpha^3}{R^3}\right]_{\rho_o}^{\rho} \overset{R=R_0}{=} \frac{3}{2}F(\rho) - \frac{3}{2}F(\rho_o) < 0.$$

[2]It should be noted that the relevant energy conditions are still violated, so the singularity theorems (see e.g., [53]) are not applicable, allowing the possibility of a bounce. Consider e.g., $8\pi(\epsilon + p_\rho)|_{R=R_0} = -3\frac{F}{R_0^3} < 0$, which violates the null, weak, dominant and strong energy condition.

The sign change in the second line is a result of $|R'|$ appearing in the square root of the metric determinant and of R'^{-1} appearing in the effective energy density and pressure. It is apparent that now gravity is repulsive not as a result of negative effective pressure, but simply because the shells are scrambled.

V. CONCLUSIONS

In this paper, we have quantized the LTB model using the assumption that the quantum dynamics of different dust shells decouple, just as in the classical case. This has allowed us to quantize only a single one of those shells, chosen to be the outermost one, and infer the behavior of the full dust cloud from the results.

Because the dust brings with it a natural time coordinate, its proper time, we have been able to ignore the usual problem of time in quantum gravity [1]. This has enabled us to construct a quantum theory for the outermost shell in analogy to conventional quantum mechanics, including unitary evolution of states. Both the choice of factor ordering and self-adjoint extension have been left open.

We have been able to show that unitarily evolving states generically avoid the classical singularity, except when the factor ordering falls into a specific range. Outside of this range, singularity avoidance holds for all self-adjoint extensions. Choosing a convenient self-adjoint extension has allowed us to examine a particular singularity-avoiding wave packet for all factor orderings. This wave packet exhibits a bounce. We have demonstrated that this bouncing behavior exhibits a robustness under quantization ambiguities similarly to singularity avoidance.

We have then investigated several properties of a quantum corrected model for gravitational collapse based on the dynamics predicted by our quantum theory: the transformation of the horizon from black hole to white hole, the lifetime of the grey hole, which turns out proportional to the third power of the ADM energy, and effective pressures facilitating the bounce. Regarding the last point, we have found that these pressures are not negative enough to make gravity repulsive in those cases where the different dust shells change their order during the bounce, but there the effective mass inside each shell is still negative exactly because of this reversed order.

When discussing these aspects of bouncing collapse, the limits of applicability of our model became apparent: using dust proper time as the time parameter and cutting off the model at the dust cloud's outermost shell has led to difficulties in determining the grey hole's lifetime and to limitations in understanding the apparent horizon.

The perhaps strongest limitation of our model is the assumption that the shells can be treated independently from each other. It is far from clear whether the shells do or do not show some emergent interaction when quantizing the full LTB model. In fact, we expect additional terms to occur in the exact Hamiltonian; after all, Hawking radiation

is not accounted for in our model. Including this radiation may by itself modify some of our results, especially in view of the lifetime we have computed (which is of the same order as the evaporation time). Perhaps it will be possible to accommodate such effects in an extended model similar to [54].

In addition, the possible occurrence of shell crossings near the bounce leaves some open questions. We have proposed a particular method to deal with them, but there might be a more elegant alternative which will also be applicable to the classical shell crossings that we have excluded from the beginning.

In spite of these limitations, we believe that our results are a first indication that quantum-gravitational effects can indeed lead to singularity avoidance in the LTB model, and that the underlying mechanism is a bounce. The degree of robustness of these features under the quantization ambiguities is certainly encouraging.

ACKNOWLEDGMENTS

T. S. thanks the Bonn-Cologne Graduate School (BCGS) for Physics and Astronomy for financial support, and Yi-Fan Wang, Nick Kwidzinski, and Jens Boos for helpful discussions.

APPENDIX A: SELF-ADJOINT EXTENSIONS OF THE HAMILTONIAN

This Appendix is devoted to finding the self-adjoint extension of the Hamiltonian (7); in this, we largely follow [55]. To start with, we choose as the domain of $\hat{H}$ all functions in $L^2(\mathbb{R}^+, R^{1-a-2b}dR)$ that are smooth and compactly supported on the half line such that the boundary term

$$W(\psi,\phi) = \langle\phi, \hat{H}\psi\rangle - \langle\hat{H}\phi, \psi\rangle = R^{-a-2b}\left(\phi^*\frac{\partial\psi}{\partial R} - \frac{\partial\phi^*}{\partial R}\psi\right)\Big|_0^\infty, \tag{A1}$$

where we take $\hat{H}$ just as a differential operator without a well-defined domain, vanishes for such a function ψ, independently of $\phi \in L^2(\mathbb{R}^+, R^{1-a-2b}dR)$. Hence, the domain of its adjoint is as large as it can be for a second order differential operator, what is called in [55] its natural domain.

To find out whether the domain of the self-adjoint Hamiltonian is unique, we need to find the deficiency indices of $\hat{H}$ as the dimensions of the solution spaces to the eigenvalue equations $\hat{H}^\dagger\psi = \pm i\psi$. The corresponding solutions are the same as the positive and negative energy stationary modes from the beginning of Sec. III; one simply has to replace E by i.

Checking for square integrability can also be done in analogy to the stationary modes: for the eigenvalue $-i$ only one mode remains and only for factor orderings $|1+a|<3$. Hence, we have for these factor orderings the deficiency index $n_- = 1$, and otherwise $n_- = 0$. Because $\hat{H}$ is real, the same has to hold for n_+. Why we have a square integrable solution to the eigenvalue equation for eigenvalue i, but none for a real eigenvalue, can be seen in the following way. The asymptotic behavior of $\phi_E^{1/2}$ for $R\to\infty$, (14) and (15), acquires an exponential component in addition to an oscillating one for $E = i$. For a specific combination of the two modes the exponentially growing parts can be made to cancel out, leaving an exponential decay towards infinity.

The deficiency indices tell us that $\hat{H}$ is essentially self-adjoint for $|1+a|\geq 3$, meaning it has a unique self-adjoint extension for those factor orderings. For $|1+a|<3$ the extension is not unique, but several choices are possible. Let us start with the former case.

The unique self-adjoint extension of an essentially self-adjoint operator is equal to its closure. The domain of this closure is given by all functions $\phi \in \mathrm{dom}\hat{H}^\dagger$ such that $W(\psi,\phi) = 0$ for all $\psi \in \mathrm{dom}\hat{H}^\dagger$. Let us first note that for every such ψ one can construct a function such that it and its derivative behave like the original function ψ (or respectively its derivative) at $R\to\infty$ or $R\to 0$, and vanish for the other boundary. It follows that we can split up the above condition $W(\psi,\phi) = 0$ into

$$w(\psi,\phi)|_{R\to 0} = 0 \quad \text{and} \quad w(\psi,\phi)|_{R\to\infty} = 0, \quad \text{where } w(\psi,\phi) = \frac{1}{2}R^{-a-2b}\left(\phi^*\frac{d\psi}{dR} - \frac{d\phi^*}{dR}\psi\right). \tag{A2}$$

To arrive at generic boundary conditions for unitarily evolving wave functions, we have to determine how a generic $\psi \in \mathrm{dom}\hat{H}^\dagger$ behaves when approaching the boundaries. Let us first consider $R\to\infty$. We know that for any $\psi \in \mathrm{dom}\hat{H}^\dagger$ both ψ and $\hat{H}\psi$ have to be square integrable. Keeping this in mind we use the identity

$$2\int_{R_0}^{R} d\tilde{R}\,\tilde{R}^{1-a-2b}(\psi^*\hat{H}\psi + \psi\hat{H}\psi^*) = \tilde{R}^{-a-2b}\frac{d|\psi|^2}{d\tilde{R}}\Big|_{R_0}^{R} - 2\int_{R_0}^{R} d\tilde{R}\tilde{R}^{1-a-2b}\left(\frac{1}{\tilde{R}}\left|\frac{d\psi}{d\tilde{R}}\right|^2 - \frac{b(1+a+2b)}{\tilde{R}^3}|\psi|^2\right),$$

where $0 < R_0 < \infty$, to argue analogously to Lemma 2.14 in [55] that $R^{-\frac{1}{2}}|\psi'|$ has to be square integrable near $R\to\infty$. In analogy to Lemma 2.13 in [55], we can then use the identities

$$\int_{R_0}^{R} d\tilde{R}\,\tilde{R}^{1-a-2b}\left(\psi^*\frac{1}{\sqrt{\tilde{R}}}\frac{d\psi}{d\tilde{R}}+\psi\frac{1}{\sqrt{\tilde{R}}}\frac{d\psi^*}{d\tilde{R}}\right)$$
$$=\tilde{R}^{\frac{1}{2}-a-2b}|\psi|^2\Big|_{R_0}^{R}-\int_{R_0}^{R} d\tilde{R}\,\tilde{R}^{1-a-2b}\frac{\frac{1}{2}-a-2b}{\tilde{R}^{\frac{3}{2}}}|\psi|^2,$$
$$2\int_{R_0}^{R} d\tilde{R}\,\tilde{R}^{1-a-2b}\left(\frac{1}{\sqrt{\tilde{R}}}\frac{d\psi^*}{d\tilde{R}}\hat{H}\psi+\frac{1}{\sqrt{\tilde{R}}}\frac{d\psi}{d\tilde{R}}\hat{H}\psi^*\right)$$
$$=\tilde{R}^{-\frac{1}{2}-a-2b}\left|\frac{d\psi}{d\tilde{R}}\right|^2+b(1+a+b)\tilde{R}^{-\frac{5}{2}-a-2b}|\psi|^2\Big|_{R_0}^{R}$$
$$+\int_{R_0}^{R} d\tilde{R}\,\tilde{R}^{\frac{1}{2}-a-2b}\left(\frac{\frac{1}{2}-a-2b}{\tilde{R}^2}\left|\frac{d\psi}{d\tilde{R}}\right|^2\right.$$
$$\left.+\frac{b(1+a+b)(\frac{5}{2}+a+2b)}{\tilde{R}^4}|\psi|^2\right)$$

to deduce that for $R\to\infty$, $R^{\frac{1}{2}-a-2b}|\psi|^2\to 0$ and $R^{-\frac{1}{2}-a-2b}|\psi'|^2\to 0$. It directly follows that $w(\psi,\phi)\to 0$ for $R\to\infty$ and any $\psi,\phi\in\mathrm{dom}\hat{H}^\dagger$, meaning the $R\to\infty$ part of (A2) is always fulfilled. This holds not only for $|1+a|\geq 3$, but for any factor ordering. We want to note that the usual pathological examples for square integrable functions not vanishing for $R\to\infty$ are excluded here by the continuity conditions on functions in $\mathrm{dom}\hat{H}^\dagger$, needed to make the expression $\hat{H}\psi$ meaningful and the above identities well defined due to the use of partial integration when deriving them.

Next we consider the boundary $R\to 0$. To this end we first note that, as mentioned previously, for a $\psi\in\mathrm{dom}\hat{H}^\dagger$ with $\hat{H}^\dagger\psi=\eta$ the function η has to be included in $L^2(\mathbb{R}^+,R^{1-a-2b}dR)$. Using the ansatz $\psi(R)=c_1(R)\phi_0^1(R)+c_2(R)\phi_0^2(R)$, where $\phi_0^{1/2}$ are the zero energy stationary modes (11), here normalized such that $w(\phi_0^1,\phi_0^2)=1$, the above equation can be inverted to give

$$\psi(R)=c_1^0\phi_0^1(R)+c_2^0\phi_0^2(R)+\phi_0^1(R)\int_{R_0}^{R} d\tilde{R}\,\tilde{R}^{1-a-2b}\phi_0^2(\tilde{R})\eta(\tilde{R})-\phi_0^2(R)\int_{\bar{R}_0}^{R} d\tilde{R}\,\tilde{R}^{1-a-2b}\phi_0^1(\tilde{R})\eta(\tilde{R}),\tag{A3}$$

$$\psi(R)'=c_1^0\phi_0^1(R)'+c_2^0\phi_0^2(R)'+\phi_0^1(R)'\int_{R_0}^{R} d\tilde{R}\,\tilde{R}^{1-a-2b}\phi_0^2(\tilde{R})\eta(\tilde{R})-\phi_0^2(R)'\int_{\bar{R}_0}^{R} d\tilde{R}\,\tilde{R}^{1-a-2b}\phi_0^1(\tilde{R})\eta(\tilde{R}),\tag{A4}$$

where c_1^0, c_2^0 and R_0, $\bar{R}_0$ are constants, the former complex and the latter on the real positive half line, and a prime denotes a differentiation with respect to R. We can now read off how ψ behaves for different factor orderings when $R\to 0$.

We first note that ϕ_0^1 is square integrable at $R=0$ for $a<2$ and at $R\to\infty$ for $a>2$, while ϕ_0^2 is square integrable at $R=0$ for $a>-4$ and at $R\to\infty$ for $a<-4$. Hence, we have to distinguish four different cases in the following, keeping in mind that we are presently only discussing the factor ordering for which $\hat{H}$ is essentially self-adjoint, $|1+a|\geq 3$.

Let us consider $a<-4$. We choose $R_0\to\infty$ and $\bar{R}_0=0$ such that the integrals in (A3) are well defined. Using the Cauchy-Schwarz inequality we can give an estimation for these terms in ψ:

$$\left|\phi_0^1(R)\int_R^\infty d\tilde{R}\,\tilde{R}^{1-a-2b}\phi_0^2(\tilde{R})\eta(\tilde{R})\right|\leq\frac{2R^{\frac{1}{2}(4+a+2b)}}{(-1-a)\sqrt{-4-a}}\left(\int_R^\infty d\tilde{R}\,\tilde{R}^{1-a-2b}|\eta(\tilde{R})|^2\right)^{\frac{1}{2}},\tag{A5}$$

$$\left|\phi_0^2(R)\int_0^R d\tilde{R}\,\tilde{R}^{1-a-2b}\phi_0^1(\tilde{R})\eta(\tilde{R})\right|\leq\frac{2R^{\frac{1}{2}(4+a+2b)}}{(-1-a)\sqrt{2-a}}\left(\int_0^R d\tilde{R}\,\tilde{R}^{1-a-2b}|\eta(\tilde{R})|^2\right)^{\frac{1}{2}},\tag{A6}$$

and analogously for $\psi(R)'$, for which $\phi_0^1(R)$ and $\phi_0^2(R)$ are replaced by $\phi_0^1(R)'$ and $\phi_0^2(R)'$, decreasing the power of R by 1. Note that the integrals on the right-hand side of the above estimates are bounded when $R\to 0$ because η is square integrable.

Furthermore, we have to set $c_2^0=0$; otherwise ψ is not square integrable at $R\to 0$. Plugging in the remaining terms pairwise into w and using the estimates (A5) and (A6), we can see that $w(\phi,\chi)$ always vanishes for any functions ϕ,χ belonging to $\mathrm{dom}\hat{H}^\dagger$ when $R\to 0$ meaning that, when keeping in mind the previous analogous result for $R\to\infty$, (A2) is always fulfilled and no additional conditions are needed.

For $a=-4$ the same conclusion holds. In this case the integral terms can respectively be estimated to behave like R^b and $R^b\sqrt{|\ln R|}$ when approaching the boundary, which still leads to $w|_{R\to 0}$ vanishing. Note that in contrast to $a<-4$ one has to choose $R_0=1$, because ϕ_0^2 is not square integrable at either boundary.

In the case of $a>2$ we choose $R_0=0$ and $\bar{R}_0\to\infty$. Apart from minor differences concerning the signs in the prefactor and the boundaries of the integral as dictated by the aforementioned choice of R_0 and $\bar{R}_0$, we can estimate the integral terms as in (A5) and (A6); most notably, the power of R remains the same. Furthermore, we choose $c_1^0=0$. Once again none of the terms contribute to $w|_{R\to 0}$. The same result emerges for the case $a=2$ ($c_1^0=0$, $R_0=0$ and $\bar{R}_0=1$), for which the integral terms can be estimated to behave like R^{3+b} and $R^{3+b}\sqrt{|\ln R|}$.

In summary, we can say that for $|1+a| \geq 3$ the domain of the essentially self-adjoint Hamiltonian is equal to $\mathrm{dom}\hat{H}^\dagger$ meaning, ignoring continuity conditions, all square integrable functions ψ for which $\hat{H}\psi$ is also square integrable.

Finally we have to consider $|1+a| < 3$. We once again utilize (A5) and (A6). Since both ϕ_0^1 and ϕ_0^2 are square integrable at $R=0$ for the factor orderings in question, we can choose $R_0 = \bar{R}_0 = 0$, and c_1^0, c_2^0 do not necessarily have to vanish. Because of ϕ_0^2, we have to consider the case where $a=-1$ on its own. Let us first restrict ourselves to $a \neq -1$. Once again the integral terms can be estimated by (A5) and (A6), with the aforementioned minor variations. The integral terms then do not contribute to w as $R \to 0$, but in contrast to the previously discussed factor orderings, ϕ_0^1 and ϕ_0^2 do.

For $a=-1$, the integral terms behave a bit differently:

$$\left|\phi_0^1(R)\int_0^R d\tilde{R}\,\tilde{R}^{2-2b}\phi_0^2(\tilde{R})\eta(\tilde{R})\right| \leq \frac{2R^{\frac{3}{2}+b}}{\sqrt{27}}\sqrt{9\ln^2 R - 6\ln R + 2}\left(\int_0^R d\tilde{R}\,\tilde{R}^{2-2b}|\eta(\tilde{R})|^2\right)^{\frac{1}{2}},$$

$$\left|\phi_0^1(R)'\int_0^R d\tilde{R}\,\tilde{R}^{2-2b}\phi_0^2(\tilde{R})\eta(\tilde{R})\right| \leq \frac{2bR^{\frac{1}{2}+b}}{\sqrt{27}}\sqrt{9\ln^2 R - 6\ln R + 2}\left(\int_0^R d\tilde{R}\,\tilde{R}^{2-2b}|\eta(\tilde{R})|^2\right)^{\frac{1}{2}},$$

$$\left|\phi_0^2(R)\int_0^R d\tilde{R}\,\tilde{R}^{2-2b}\phi_0^1(\tilde{R})\eta(\tilde{R})\right| \leq \frac{2}{\sqrt{3}}R^{\frac{3}{2}+b}|\ln R|\left(\int_0^R d\tilde{R}\,\tilde{R}^{2-2b}|\eta(\tilde{R})|^2\right)^{\frac{1}{2}},$$

$$\left|\phi_0^2(R)'\int_0^R d\tilde{R}\,\tilde{R}^{2-2b}\phi_0^1(\tilde{R})\eta(\tilde{R})\right| \leq \frac{2}{\sqrt{3}}R^{\frac{1}{2}+b}|b\ln R + 1|\left(\int_0^R d\tilde{R}\,\tilde{R}^{2-2b}|\eta(\tilde{R})|^2\right)^{\frac{1}{2}}.$$

Despite the differences to previous factor orderings, the results are identical: only ϕ_0^1 and ϕ_0^2 contribute to w as $R \to 0$.

Combining the above with our previous result for the behavior of ψ for $R \to \infty$, we can give an asymptotic expansion for any $\psi \in \mathrm{dom}\hat{H}^\dagger$ for $R \to 0$ as

$$\psi(R) = c_1^0\phi_0^1(R) + c_2^0\phi_0^2(R) + \tilde{\psi}_0(R),$$

where c_1^0, c_2^0 are arbitrary constants, and $\tilde{\psi}_0$ does not contribute to $w|_{R\to 0}$. $w|_{R\to\infty}$ always vanishes, and hence there we have $\psi = \tilde{\psi}_\infty$. Note that the asymptotic expansion of the derivative is equal to the derivative of the asymptotic expansion above.

This allows us to determine self-adjoint extensions for $\hat{H}$ by using Theorem 4.24 of [55], where the procedure we employ below is called the "asymmetry form method." A more pedagogical introduction to this method can be found in [41].

To start with, we consider the asymmetry form

$$\Delta(\psi) = W(\psi,\psi) = -w(\psi,\psi)|_{R\to 0} = c_1^{0*}c_2^0 - c_2^{0*}c_1^0,$$

where we have used that ϕ_0^1, ϕ_0^2 are real and normalized such that $w(\phi_0^1,\phi_0^2) = 1$. The next step is then to diagonalize the asymmetry form, which in our case can be achieved by defining $c_+ = \frac{1}{2}(-c_1^0 + ic_2^0)$ and $c_- = \frac{1}{2}(c_1^0 + ic_2^0)$ such that

$$\Delta(\psi) = 2i(|c_+|^2 - |c_-|^2).$$

All self-adjoint extensions of $\hat{H}$ can then be given by the condition

$$c_- = e^{i\theta}c_+, \tag{A7}$$

where $\theta \in [0, 2\pi)$.

To check whether a given $\psi \in \mathrm{dom}\hat{H}^\dagger$ fulfills this condition for a given θ, we need to extract the constants $c_\pm$ from the asymptotic expansion of ψ. To this end, we note

$$w(\psi,\phi_0^1)|_{R\to 0} = -c_2^0,$$
$$w(\psi,\phi_0^2)|_{R\to 0} = c_1^0.$$

This allows us to write the condition (A7) as

$$-(1+e^{i\theta})R^{2+a}\frac{d}{dR}R^{-(1+a+b)}\psi\Big|_{R\to 0} = i(1-e^{i\theta})R^{-a}\frac{d}{dR}R^{-b}\psi\Big|_{R\to 0} \tag{A8}$$

for $a \neq -1$, and for $a=-1$ as

$$-(1+e^{i\theta})R\ln^2 R\frac{d}{dR}\frac{R^{-b}}{\ln R}\psi\Big|_{R\to 0} = i(1-e^{i\theta})R\frac{d}{dR}R^{-b}\psi\Big|_{R\to 0}. \tag{A9}$$

Finally we note that θ can, of course, be chosen differently for each factor ordering. We thus change θ according to $\theta \to -\theta + \pi$ for $a > -1$, allowing us to rewrite (A8) as

$$-(1+e^{i\theta})R^{1-|1+a|}\frac{d}{dR}R^{-\frac{1}{2}(1+a-|1+a|+2b)}\psi\Big|_{R\to 0} = i(1-e^{i\theta})R^{1+|1+a|}\frac{d}{dR}R^{-\frac{1}{2}(1+a+|1+a|+2b)}\psi\Big|_{R\to 0}. \tag{A10}$$

It turns out that this form of the boundary conditions works best for our stationary modes. This concludes our discussion of the self-adjoint extensions of the Hamiltonian.

APPENDIX B: APPLYING BOUNDARY CONDITIONS TO THE STATIONARY MODES

We want to enforce the boundary conditions (19) and (20), which correspond to the different self-adjoint extensions of the Hamiltonian for the positive energy stationary modes ϕ_E^1 and ϕ_E^2. Recall that only factor orderings with $|1+a|<3$ are relevant here. First we will consider $a \neq -1$.

We start with ϕ_E^1 and compute

$$\begin{aligned}
R^{1-|1+a|}\frac{d}{dR}R^{-\frac{1}{2}(1+a-|1+a|+2b)}\phi_E^1 &= -\sqrt{2E}R^{\frac{1}{2}(3-|1+a|)}\left(\cos\left(\frac{\pi}{3}|1+a|\right)J_{1-\frac{1}{3}|1+a|}\left(\frac{2}{3}\sqrt{2E}R^{\frac{3}{2}}\right)\right.\\
&\quad\left.+\sin\left(\frac{\pi}{3}|1+a|\right)Y_{1-\frac{1}{3}|1+a|}\left(\frac{2}{3}\sqrt{2E}R^{\frac{3}{2}}\right)\right)\\
&\overset{R\to 0}{\sim} -\frac{3\cos(\frac{\pi}{3}|1+a|)}{\Gamma(2-\frac{1}{3}|1+a|)}\left(\frac{1}{3}\sqrt{2E}\right)^{2-\frac{1}{3}|1+a|}R^{3-|1+a|}\\
&\quad+\frac{3}{\pi}\sin\left(\frac{\pi}{3}|1+a|\right)\Gamma\left(1-\frac{1}{3}|1+a|\right)\left(\frac{1}{3}\sqrt{2E}\right)^{\frac{1}{3}|1+a|},\\
R^{1+|1+a|}\frac{d}{dR}R^{-\frac{1}{2}(1+a+|1+a|+2b)}\phi_E^1 &= -\sqrt{2E}R^{\frac{1}{2}(3+|1+a|)}J_{1+\frac{1}{3}|1+a|}\left(\frac{2}{3}\sqrt{2E}R^{\frac{3}{2}}\right)\\
&\overset{R\to 0}{\sim} -\frac{3(\frac{1}{3}\sqrt{2E})^{2+\frac{1}{3}|1+a|}}{\Gamma(2+\frac{1}{3}|1+a|)}R^{3+|1+a|},
\end{aligned}$$

where we have used several well-known identities of the Bessel functions and their derivatives, which can be found e.g., in [42], along with their asymptotic behavior. Inserting ϕ_E^1 on its own into (19) would thus lead to $e^{i\theta}+1=0$. ϕ_E^1 is hence viable for $\theta=\pi$, but for other self-adjoint extensions we have to consider more general linear combinations of the two modes.

For ϕ_E^2 we proceed along the same lines as for ϕ_E^1 and compute

$$\begin{aligned}
R^{1-|1+a|}\frac{d}{dR}R^{-\frac{1}{2}(1+a-|1+a|+2b)}\phi_E^2 &= \sqrt{2E}R^{\frac{1}{2}(3-|1+a|)}\left(\sin\left(\frac{\pi}{3}|1+a|\right)J_{1-\frac{1}{3}|1+a|}\left(\frac{2}{3}\sqrt{2E}R^{\frac{3}{2}}\right)\right.\\
&\quad\left.-\cos\left(\frac{\pi}{3}|1+a|\right)Y_{1-\frac{1}{3}|1+a|}\left(\frac{2}{3}\sqrt{2E}R^{\frac{3}{2}}\right)\right)\\
&\overset{R\to 0}{\sim} \frac{3\sin(\frac{\pi}{3}|1+a|)}{\Gamma(2-\frac{1}{3}|1+a|)}\left(\frac{1}{3}\sqrt{2E}\right)^{2-\frac{1}{3}|1+a|}R^{3-|1+a|}\\
&\quad+\frac{3}{\pi}\cos\left(\frac{\pi}{3}|1+a|\right)\Gamma\left(1-\frac{1}{3}|1+a|\right)\left(\frac{1}{3}\sqrt{2E}\right)^{\frac{1}{3}|1+a|},\\
R^{1+|1+a|}\frac{d}{dR}R^{-\frac{1}{2}(1+a+|1+a|+2b)}\phi_E^2 &= -\sqrt{2E}R^{\frac{1}{2}(3+|1+a|)}Y_{1+\frac{1}{3}|1+a|}\left(\frac{2}{3}\sqrt{2E}R^{\frac{3}{2}}\right)\\
&\overset{R\to 0}{\sim} \frac{3}{\pi}\Gamma\left(1+\frac{1}{3}|1+a|\right)\left(\frac{1}{3}\sqrt{2E}\right)^{-\frac{1}{3}|1+a|},
\end{aligned}$$

On its own, ϕ_E^2 would only be able to fulfill (19) for a single specific energy, but since it is not square integrable, it does not admit an interpretation as a bound state. As noted above, only a specific linear combination $A\phi_E^1+B\phi_E^2$, $A\neq 0$, is permissible under (19):

$$-(1+e^{i\theta})\Gamma\left(1-\frac{1}{3}|1+a|\right)\left(\frac{1}{3}\sqrt{2E}\right)^{\frac{1}{3}|1+a|}\times\left(A\sin\left(\frac{\pi}{3}|1+a|\right)+B\cos\left(\frac{\pi}{3}|1+a|\right)\right)=i(1-e^{i\theta})\Gamma\left(1+\frac{1}{3}|1+a|\right)\left(\frac{1}{3}\sqrt{2E}\right)^{-\frac{1}{3}|1+a|}B.$$

For $\theta=\pi$ the above implies $B=0$, and hence we see that ϕ_E^1 and only ϕ_E^1 is viable for this self-adjoint extension. With $\theta\neq\pi$ we continue and arrive at

$$A\sin\left(\frac{\pi}{3}|1+a|\right)+B\cos\left(\frac{\pi}{3}|1+a|\right)=-\tan\frac{\theta}{2}\,\frac{\Gamma(1+\frac{1}{3}|1+a|)}{\Gamma(1-\frac{1}{3}|1+a|)}\left(\frac{1}{3}\sqrt{2E}\right)^{-\frac{2}{3}|1+a|}B,$$

and hence the positive energy stationary mode permitted by (19) is

$$-\tan\frac{\theta}{2}\,\frac{\Gamma(1+\frac{1}{3}|1+a|)}{\Gamma(1-\frac{1}{3}|1+a|)}\left(\frac{1}{3}\sqrt{2E}\right)^{-\frac{2}{3}|1+a|}\phi_E^1-\cos\left(\frac{\pi}{3}|1+a|\right)\phi_E^1+\sin\left(\frac{\pi}{3}|1+a|\right)\phi_E^2.$$

Finally we want to consider the case $a=-1$. Plugging $A\phi_E^1+B\phi_E^2$ into (20) and a straightforward calculation leads to

$$(1+e^{i\theta})\left(A+\frac{2B}{\pi}\ln\left(\frac{2}{3}\sqrt{2E}\right)\right)=i(1-e^{i\theta})\frac{3B}{\pi}.$$

As is apparent, for $\theta=\pi$ we once again have as our permitted mode ϕ_E^1, and for other factor orderings

$$\left(\frac{3}{\pi}\tan\frac{\theta}{2}-\frac{2}{\pi}\ln\left(\frac{2}{3}\sqrt{2E}\right)\right)\phi_E^1+\phi_E^2.$$

APPENDIX C: MINIMAL RADIUS FOR THE FULL WAVE PACKET

The expectation value of the minimal radius for the full wave packet (29) can be computed as

$$\begin{aligned}\bar{R}(\tau=0)&=\int_0^\infty dR\,R^{1-a-2b}R|\Psi(R,\tau=0)|^2\\&=\lambda^{\frac{1}{3}}\frac{2^{\kappa+\frac{1}{3}}\pi}{3^{\frac{1}{3}}}\frac{\csc(\frac{\pi}{6}(|a+1|-3\kappa+2))\Gamma\left(\frac{|a+1|}{6}+\frac{\kappa}{2}+1\right)}{\Gamma(\frac{2}{3})\Gamma(\kappa+1)\Gamma\left(\frac{|a+1|}{6}-\frac{\kappa}{2}\right)}\\&\times\left[\Gamma\left(\frac{|a+1|}{3}+\frac{4}{3}\right)\Gamma\left(\frac{|a+1|}{6}-\frac{\kappa}{2}\right){}_3\tilde{F}_2\left(\frac{4}{3},\frac{|a+1|}{6}+\frac{\kappa}{2}+1,\frac{|a+1|}{3}+\frac{4}{3};\frac{|a+1|}{6}-\frac{\kappa}{2}+\frac{4}{3},\frac{|a+1|}{3}+1;-1\right)\right.\\&\left.+3\Gamma\left(\frac{2}{3}\right)\Gamma\left(\kappa+\frac{2}{3}\right){}_3\tilde{F}_2\left(\kappa+\frac{2}{3},-\frac{|a+1|}{6}+\frac{\kappa}{2}+1,\frac{|a+1|}{6}+\frac{\kappa}{2}+1;-\frac{|a+1|}{6}+\frac{\kappa}{2}+\frac{2}{3},\frac{|a+1|}{6}+\frac{\kappa}{2}+\frac{2}{3};-1\right)\right],\end{aligned}$$

where ${}_3\tilde{F}_2$ are regularized hypergeometric functions. The function $g(a,\kappa)$ follows from comparison of the above with the expression $\bar{R}(\tau=0)=\lambda^{\frac{1}{3}}g(a,\kappa)$. It is obvious that it intricately depends on both a and κ.

APPENDIX D: TRANSITION PROBABILITIES

The full expression for the probability for the transition from collapse to grey hole state, as well as from collapse to expansion is rather complicated,

$$\begin{aligned}\frac{P_{\mathrm{C}\to\mathrm{E}}}{P_{\mathrm{C}\to\mathrm{GH}}}&=\frac{\int_{-\infty}^{-\tau_{\mathrm{AH}}}d\tau_-\int_{\tau_{\mathrm{AH}}}^{\infty}d\tau_+W(\tau_-,\tau_+)}{\int_{-\infty}^{-\tau_{\mathrm{AH}}}d\tau_-\int_{-\tau_{\mathrm{AH}}}^{\tau_{\mathrm{AH}}}d\tau_+W(\tau_-,\tau_+)}\\&=\frac{\frac{2^{\frac{2}{3}|1+a|}}{\frac{2}{3}|1+a|+1}{}_2F_1\left(\frac{1}{2},1;\frac{|1+a|}{3}+\frac{3}{2};-\frac{\lambda^2}{4\tau_{\mathrm{AH}}^2}\right)-1}{1-\left(\frac{4\tau_{\mathrm{AH}}^2}{\lambda^2}+1\right)^{\frac{|1+a|}{3}}\left(1+\frac{2\sqrt{\pi}\tau_{\mathrm{AH}}\Gamma(\frac{|1+a|}{3}+\frac{1}{2})}{\lambda\Gamma(\frac{|1+a|}{3})}-\frac{8\tau_{\mathrm{AH}}^2|1+a|}{3\lambda^2}{}_2F_1\left(\frac{1}{2},\frac{|1+a|}{3}+1;\frac{3}{2};-\frac{4\tau_{\mathrm{AH}}^2}{\lambda^2}\right)\right)}.\end{aligned}\tag{D1}$$

Keeping in mind that $\frac{\tau_{\rm AH}}{\lambda}$ is roughly proportional to $\bar{E}^2$ for a fixed, we can approximate the result for high energies. To this end, we note that asymptotically the Gauss hypergeometric function ${}_2F_1$ behaves like [42]

$$ {}_2F_1(a,b;c;z) \approx \frac{\Gamma(c)\Gamma(b-a)}{\Gamma(b)\Gamma(c-a)}(-z)^{-a} + \frac{\Gamma(c)\Gamma(a-b)}{\Gamma(a)\Gamma(c-b)}(-z)^{-b} \quad \text{for } |z| \to \infty, $$

$$ {}_2F_1(a,b;c;z) \approx 1 + \frac{ab}{c}z \quad \text{for } |z| \to 0. $$

Applying this to (D1) above gives

$$ \frac{P_{\rm C\to E}}{P_{\rm C\to GH}} \approx \frac{(2\frac{\tau_{\rm AH}}{\lambda})^{-\frac{2}{3}|1+a|}}{\frac{2}{3}|1+a|+1}. $$

The same approximation can be applied to the transition probability from grey hole to expanding state,

$$ \begin{aligned} P_{\rm GH\to E} &= \frac{\int_{-\tau_{\rm AH}}^{\tau_{\rm AH}} d\tau_- \int_{\tau_{\rm AH}}^{\infty} d\tau_+ W(\tau_-,\tau_+)}{\int_{-\tau_{\rm AH}}^{\tau_{\rm AH}} d\tau_- \int_{-\infty}^{\infty} d\tau_+ W(\tau_-,\tau_+)} \\ &= \frac{1}{2} + \frac{\Gamma(\frac{1}{3}|a+1|)}{4\sqrt{\pi}\Gamma(\frac{1}{3}|a+1|+\frac{1}{2})}\frac{\lambda}{\tau_{\rm AH}}\left(1-\left(1+\frac{4\tau_{\rm AH}^2}{\lambda^2}\right)^{-\frac{1}{3}|a+1|}\right) \\ &\quad - \frac{2\Gamma(\frac{1}{3}|a+1|+1)}{\sqrt{\pi}\Gamma(\frac{1}{3}|a+1|+\frac{1}{2})}\frac{\tau_{\rm AH}}{\lambda}\,{}_2F_1\left(\frac{1}{2},\frac{1}{3}|a+1|+1;\frac{3}{2};-\frac{4\tau_{\rm AH}^2}{\lambda^2}\right) \qquad \text{(D2)} \\ &\approx \frac{\Gamma(\frac{1}{3}|a+1|)}{4\sqrt{\pi}\Gamma(\frac{1}{3}|a+1|+\frac{1}{2})}\frac{\lambda}{\tau_{\rm AH}}. \qquad \text{(D3)} \end{aligned} $$

Note that this approximation for high energies only applies when $a \neq -1$, otherwise (D3) behaves like $\frac{\lambda}{\tau_{\rm AH}}\ln(2\frac{\tau_{\rm AH}}{\lambda})$.

[1] C. Kiefer, *Quantum Gravity*, 3rd ed. (Oxford University Press, Oxford, 2012).
[2] V. Frolov and G. Vilkovisky, Phys. Lett. B **106**, 307 (1981).
[3] P. Hájíček and C. Kiefer, Nucl. Phys. **B603**, 531 (2001); P. Hájíček, *ibid.* **B603**, 555 (2001).
[4] P. Hájíček and C. Kiefer, Int. J. Mod. Phys. D **10**, 775 (2001).
[5] M. Ambrus and P. Hájíček, Phys. Rev. D **72**, 064025 (2005).
[6] P. Hájíček, in *Quantum Gravity: From Theory to Experimental Search*, edited by D. Giulini, C. Kiefer, and C. Lämmerzahl (Springer, Berlin, 2003), pp. 255–299; C. Kiefer, arXiv:1512.08346.
[7] I. Albarran, M. Bouhmadi-López, C. Kiefer, J. Marto, and P. Vargas Moniz, Phys. Rev. D **94**, 063536 (2016).
[8] C. Kiefer, N. Kwidzinski, and D. Piontek, arXiv:1903.04391.
[9] C. Rovelli and F. Vidotto, Int. J. Mod. Phys. D **23**, 1442026 (2014).
[10] A. Ashtekar, J. Phys. Conf. Ser. **189**, 012003 (2009).
[11] A. Ashtekar and M. Bojowald, Classical Quantum Gravity **22**, 3349 (2005).
[12] C. Bambi, D. Malafarina, and L. Modesto, Eur. Phys. J. C **74**, 2767 (2014).
[13] C. Bambi, D. Malafarina, and L. Modesto, Phys. Rev. D **88**, 044009 (2013).
[14] C. Barceló, R. Carballo-Rubio, and L. J. Garay, Int. J. Mod. Phys. D **23**, 1442022 (2014).
[15] C. Barceló, R. Carballo-Rubio, L. J. Garay, and G. Jannes, Classical Quantum Gravity **32**, 035012 (2015).
[16] H. M. Haggard and C. Rovelli, Phys. Rev. D **92**, 104020 (2015).
[17] C. Barceló, R. Carballo-Rubio, and L. J. Garay, Classical Quantum Gravity **34**, 105007 (2017).
[18] M. Christodoulou, C. Rovelli, S. Speziale, and I. Vilensky, Phys. Rev. D **94**, 084035 (2016).
[19] M. Christodoulou and F. D'Ambrosio, arXiv:1801.03027.
[20] D. Malafarina, Universe **3**, 48 (2017).
[21] A. Krasiński, *Inhomogeneous Cosmological Models* (Cambridge University Press, Cambridge, England, 1997).
[22] C. Vaz, L. Witten, and T. P. Singh, Phys. Rev. D **63**, 104020 (2001).
[23] C. Kiefer, J. Müller-Hill, and C. Vaz, Phys. Rev. D **73**, 044025 (2006).
[24] C. Vaz, C. Kiefer, T. P. Singh, and L. Witten, Phys. Rev. D **67**, 024014 (2003).
[25] C. Kiefer, J. Müller-Hill, T. P. Singh, and C. Vaz, Phys. Rev. D **75**, 124010 (2007).
[26] R. Banerjee, C. Kiefer, and B. R. Majhi, Phys. Rev. D **82**, 044013 (2010).
[27] C. Vaz and L. Witten, Phys. Rev. D **64**, 084005 (2001).

[28] M. Bojowald, Phys. Rev. Lett. **95**, 061301 (2005).
[29] V. Husain and O. Winkler, Classical Quantum Gravity **22**, L127 (2005).
[30] M. Bojowald, T. Harada, and R. Tibrewala, Phys. Rev. D **78**, 064057 (2008).
[31] M. Bojowald, J. D. Reyes, and R. Tibrewala, Phys. Rev. D **80**, 084002 (2009).
[32] L. B. Szabados, Living Rev. Relativity **12**, 4 (2009).
[33] B. C. Nolan, Classical Quantum Gravity **20**, 575 (2003).
[34] H. J. Seifert, Gen. Relativ. Gravit. **10**, 1065 (1979).
[35] E. Poisson, *A Relativist's Toolkit: The Mathematics of Black-Hole Mechanics* (Cambridge University Press, Cambridge, England, 2004).
[36] J. D. Brown and K. V. Kuchař, Phys. Rev. D **51**, 5600 (1995).
[37] D. Giulini and C. Kiefer, Phys. Lett. A **193**, 21 (1994).
[38] K. Giesel, J. Tambornino, and T. Thiemann, Classical Quantum Gravity **27**, 105013 (2010).
[39] H. Maeda, Classical Quantum Gravity **32**, 235023 (2015).
[40] M. Abramowitz and I. A. Stegun, *Handbook of Mathematical Functions with Formulas, Graphs, and Mathematical Tables*, 9th Dover printing, 10th gpo printing ed. (Dover, New York, 1964).
[41] T. Fülöp, SIGMA **3**, 107 (2007).
[42] NIST Digital Library of Mathematical Functions, Release 1.0.21 of 2018-12-15, edited by F. W. J. Olver, A. B. Olde Daalhuis, D. W. Lozier, B. I. Schneider, R. F. Boisvert, C. W. Clark, B. R. Miller, and B. V. Saunders, http://dlmf.nist.gov/.
[43] G. Arfken and H. Weber, *Mathematical Methods for Physicists*, 6th ed. (Academic Press, Boston, 2005).
[44] I. S. Gradshteyn, A. Jeffrey, and I. M. Ryzhik, *Table of Integrals, Series, and Products*, 5th ed. (Academic Press, Boston, 1996).
[45] M. P. Dąbrowski, C. Kiefer, and B. Sandhöfer, Phys. Rev. D **74**, 044022 (2006).
[46] F. G. Alvarenga, J. C. Fabris, N. A. Lemos, and G. A. Monerat, Gen. Relativ. Gravit. **34**, 651 (2002).
[47] P. Joshi, *Gravitational Collapse and Spacetime Singularities* (Cambridge University Press, Cambridge, England, 2007).
[48] C. Barceló, R. Carballo-Rubio, and L. J. Garay, J. High Energy Phys. 01 (2016) 157.
[49] W. Israel, Phys. Rev. **153**, 1388 (1967).
[50] E. H. Hauge and J. A. Støvneng, Rev. Mod. Phys. **61**, 917 (1989).
[51] V. S. Olkhovsky, E. Recami, and A. K. Zaichenko, Europhys. Lett. **70**, 712 (2005).
[52] C. Kiefer and J. Louko, Ann. Phys. (Berlin) **8**, 67 (1999).
[53] S. W. Hawking and G. F. R. Ellis, *The Large Scale Structure of Space-Time* (Cambridge University Press, Cambridge, England, 1973).
[54] C. Kiefer, J. Marto, and P. Vargas Moniz, Ann. Phys. (Berlin) **18**, 722 (2009).
[55] D. M. Gitman, I. V. Tyutin, and B. L. Voronov, *Self-adjoint Extensions in Quantum Mechanics*, Progress in Mathematical Physics (Birkhäuser, Basel, 2012).